Available online at www.sciencedirect.com
ScienceDirect
Lithos 90 (2006) 161–186
LITHOS
www.elsevier.com/locate/lithos

Magmatic relationships and ages of Caribbean Island arc tholeiites, boninites and related felsic rocks, Dominican Republic

J. Escuder Viruete [a,d,*], A. Díaz de Neira [b], P.P. Hernáiz Huerta [b], J. Monthel [c], J. García Senz [b], M. Joubert [c], E. Lopera [d], T. Ullrich [e], R. Friedman [e], J. Mortensen [e], A. Pérez-Estaún [f]

[a] *Depto. Petrología y Geoquímica, Universidad Complutense. 28040 Madrid, Spain*
[b] *INYPSA, C. Velázquez-69, 1°, 28001 Madrid, Spain*
[c] *BRGM, Av. C. Guillemin, 45060 Orléans, France*
[d] *IGME, C. Ríos Rosas-23, 28003 Madrid, Spain*
[e] *Pacific Centre for Isotopic and Geochemical Research, University of British Columbia, 6339 Stores Road Vancouver, BC, Canada V6T 1Z4*
[f] *I.C.T. Jaume Almera-CSIC, Lluís Solé i Sabarís s/n. 08028 Barcelona, Spain*

Received 28 June 2005; accepted 10 February 2006
Available online 2 May 2006

Abstract

Located in the Cordillera Oriental of the Dominican Republic, the Early Cretaceous Los Ranchos Fm (LRF) comprises a >3-km thick sequence of volcanic and volcaniclastic rocks with variable geochemical characteristics, which is intruded by tonalite batholiths, minor gabbro/diorite plutons and mafic dykes. From top to bottom, three main stratigraphic units have been mapped: upper basaltic, intermediate rhyodacitic and lower basaltic. Combined detailed mapping, stratigraphy, geochemistry, Rb–Sr/Sm–Nd isotopic studies and U–Pb/Ar–Ar geochronology show that the mafic rocks of the LRF include boninites and LREE-depleted island arc tholeiites (IAT) in the lower unit, both which appear genetically related, whereas normal IAT occur in the upper unit. The source for these rocks is thought to reflect variably depleted mantle, overprinted by a subduction zone component. Contemporaneous Aptian U–Pb zircon ages were obtained for a rhyodacite from the intermediate unit (116.0±0.8 Ma) and a tonalite of the Zambrana batholith (115.5±0.3 Ma) that intrudes the LRF. The similarity of trace element signatures in both units argues for genetic link between the felsic volcanics of the LRF and the tonalite plutonism. Low-K rhyolites and tonalite batholiths are interpreted as products of secondary melting at the base of thickened early arc crust. $^{40}Ar/^{39}Ar$ plateau ages of hornblende in most tonalites are Albian (109–106 Ma) and interpreted as final cooling ages, prior to unroofing and growth of unconformable overlying reef limestones of the Hatillo Fm (112–100 Ma). The LREE-depleted IAT and boninites of lower basaltic unit are interpreted to have formed during subduction zone initiation in the Caribbean Island arc, and the normal IAT of the upper unit are thought to represent the subsequent establishment of the volcanic front.

Keywords: Island arc tholeiite; Boninite; Felsic rocks; U–Pb ages; Caribbean Island arc

1. Introduction

Boninites and low-Ti, high-Mg tholeiitic-related rocks have been identified in many Western Pacific intraoceanic arcs (Meijer, 1980; Bloomer and Hawkins,

* Corresponding author. Depto. Petrología y Geoquímica, Universidad Complutense. 28040 Madrid, Spain. Tel.: +34 91 7287242.
E-mail address: escuder@geo.ucm.es (J. Escuder Viruete).

0024-4937/$ - see front matter © 2006 Elsevier B.V. All rights reserved.
doi:10.1016/j.lithos.2006.02.001

1987; Crawford et al., 1989 and references therein). Typically, the primitive composition of boninitic lavas combined with their high large ion lithophile/high field strength elements (LILE/HFSE) ratios are thought to be generated from a depleted mantle wedge to which a fluid or melt component has been added (Crawford et al., 1989; Van der Laan et al., 1992; Pearce et al., 1992; Bédard, 1999). For this reason, models for the generation of boninitic lavas invoke melting of depleted mantle at shallow depths during atypical subduction conditions, such as initiation of subduction or ridge subduction. In the Western Pacific island arcs, the eruptive setting of Tertiary boninites has been spatially restricted to forearc regions, mostly associated with early arc development (Pearce et al., 1992; Bloomer et al., 1995; Taylor and Nesbitt, 1995). Therefore, boninites are often considered as important, unambiguous, paleogeodynamic markers of incipient subduction in a forearc setting. In this respect, ancient boninites are interpreted to have been generated by processes similar to those in modern settings, such as supra-subduction zones (McCulloch and Gamble, 1991; MacLachlan and Dunning, 1998), forearcs (Brown and Jenner, 1989; Bédard et al., 1998), or arcs at an early stage of development (Clift and Dixon, 1998; Spadea and Scarrow, 2000).

Located in the Cordillera Oriental of the Dominican Republic, the Early Cretaceous Los Ranchos Fm (LRF) is part of the oldest and chemically most primitive island arc in the Caribbean Basin (Donnelly et al., 1990; Lewis and Draper, 1990; Kesler et al., 1990, 2005; Lewis et al., 2000, 2002). The Neogene tectonics that affect whole Hispaniola Island followed by uplift and unroofing by erosion of these rocks provide access to crustal levels, not exposed in modern equivalents. Therefore, the tectonomagmatic evolution of arc-related volcanic, volcaniclastic and sedimentary sequences of the LRF, as well as related gabbroic to tonalitic intrusives, can provide important constraints on initiation of intra-oceanic subduction and development of the Caribbean Island arc. Further, these rocks are particularly important to constraint tectonic models for the Caribbean plate during the Early Cretaceous.

As part of the Cartographic Program of the Dominican Republic funded by the European Union (SYSMIN project) an integrated study of detailed mapping, stratigraphy, geochemistry, Sm–Nd isotopic studies and U–Pb/Ar–Ar geochronology of the LRF has been carried out. This study showed that mafic rocks of the LRF include boninites and LREE-depleted island arc tholeiites (IAT) in the lower stratigraphic unit, both of which appear genetically related, whereas normal IAT occur in the upper unit. Furthermore, a genetic link between volcanic and plutonic felsic rocks can be demonstrated, and this is interpreted to represent processes at different crustal levels in the same arc. Finally, field and stratigraphic relationships in the volcanic rocks provide support for tectonomagmatic models of subduction zone initiation and Caribbean Island arc development based on geochemical arguments.

2. Geological setting

Located in the northern margin of the Caribbean plate (Fig. 1), the tectonic collage of Hispaniola Island results from the WSW to SW-directed oblique-convergence of the continental margin of the North American plate with the Cretaceous Greater Antilles island-arc system, which began in Eocene to early Miocene times and continues today (Donnelly et al., 1990; Lewis and Draper, 1990; Draper et al., 1994; Mann, 1999). Hispaniola has been divided into tectonostratigraphic terranes based on their different geological history (Mann et al., 1991), tectonically juxtaposed by post-Eocene/Oligocene strike–slip, WNW–ESE fault zones. These are the Septentrional (SFZ), Hispaniola (HFZ), Bonao–La Guácara (BGFZ), San Juan–Restauración (SJRFZ) and Enrriquillo–Plantain Garden (EPGFZ) fault zones (Fig. 1). The Mesozoic arc-related rocks are regionally overlain by upper Eocene to Holocene sedimentary rocks that post-date island-arc magmatic activity and record the oblique arc–continent collision in the north, as well as active subduction in the southern Hispaniola margin (Dolan et al., 1998; Mann, 1999). Collisional processes have led to deformation in the forearc, intra-arc and backarc volcano-sedimentary basins, and upper Miocene–Recent topographic uplift in Hispaniola.

3. Previous work

The Early Cretaceous LRF is part of the primitive Caribbean Island arc (Donnelly et al., 1990; Kesler et al., 1990, 2005; Lebrón and Perfit, 1994; Draper et al., 1994; Jolly et al., 1998; Kerr et al., 1999; Lewis et al., 2000, 2002). Donnelly et al. (1990) used the term primitive to describe the LRF and similar Caribbean volcanic rock suites that: (1) formed at an early stage in the evolution of the island arc; (2) were not derived by differentiation from any other magma type; and (3) in which LILE were not enriched during differentiation. Previous workers, beginning with Bowin (1975), described volcanic rocks of the LRF as spilites and keratophyres, forming a 100-km-long belt that extends

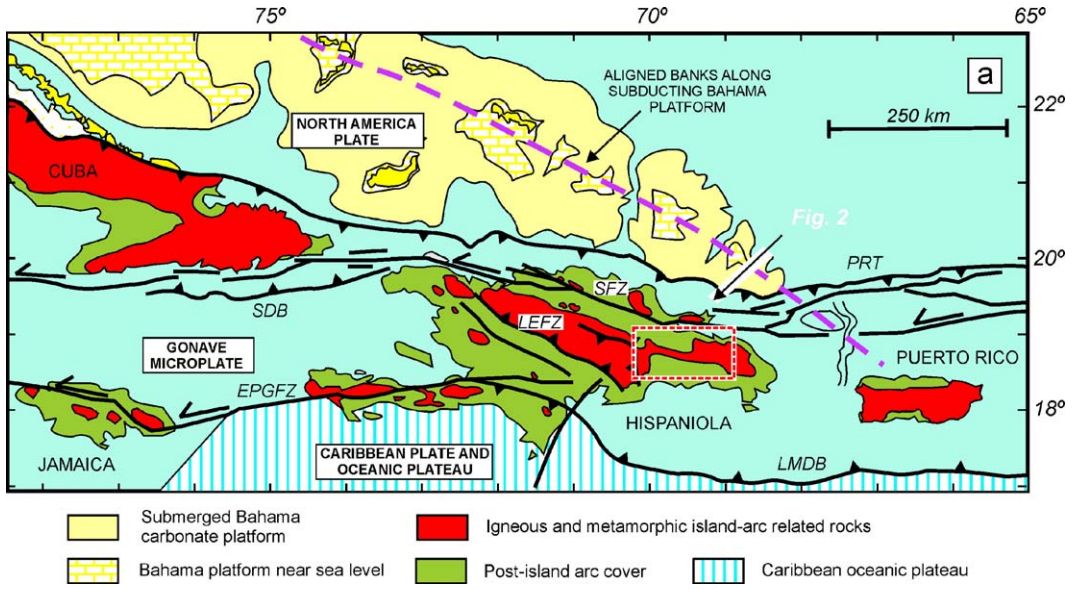

Fig. 1. Map of the northeastern Caribbean plate margin modified from Dolan et al. (1998). OFZ = Oriente Fault Zone; SDB = Santiago deformed belt; NHDB = North Hispaniola deformed belt; PRT = Puerto Rico trench; LMDB = Los Muertos deformed belt; EPGFZ = Enriquillo–Plantain Garden fault zone; SFZ = Septentrional fault zone; HFZ = Hispaniola fault zone; BGFZ = Bonao–La Guácara fault zone; SJRFZ = San Juan–Restauración fault zone. Box shows map of the eastern Dominican Republic in Fig. 2.

eastward from the Cotui-Pueblo Viejo area to Miches on the south shore of the Samana Bay (Figs. 1 and 2). This terminology for altered volcanic rocks was abandoned by Kesler et al. (1990) and the LRF rocks referred as andesite and dacite, on basis of phenocryst assemblage and whole-rock geochemistry. They report a bimodal silica distribution for volcanic rocks corresponding to basaltic andesite and dacite. Regional data of the geology and geochemistry of the LRF are also included in Bourdon (1985), Kesler et al. (1977, 2003), Lebrón and Perfit (1994), Lewis et al. (2002) and unpublished geological maps of the Dirección General de Minería at Santo Domingo.

In the Pueblo Viejo mine area, the LRF was divided into four members (Mb) by Kesler et al. (1977) and later modified to six members by Kesler et al. (1990) upon extending the unit to the area of Cotuí-Cevicos. These authors define a basal unit consisting largely of locally pillowed, spilitized mafic flows (Cotuí Mb) and acid flows, minor tuffs and subvolcanic intrusions (Quita Sueño Mb), which are overlain by basal debris flows, volcanic sandstone and lithic tuff (Meladito Fragmental Mb), and unpillowed spilitized mafic flows (Platanal and Naviza Mbs), locally amygdaloidal and agglomeratic, with clinopyroxene and plagioclase phenocrysts. The Meladito and Platanal Mb are cut by the Zambrana Fragmental and the Pueblo Viejo Maar-Diatreme Mb, which formed in a phreatomagmatic eruption during a late stage of volcanism, when the volcano was emergent (Kesler et al., 1990, 2003). Pueblo Viejo Mb has a thin-bedded sequence of carbonaceous sandstone and siltstone, with Early Cretaceous-age terrestrial plant fossils (Kesler et al., 1990). Model ages from Pb-isotope analyses of Los Ranchos volcanic rocks are between 135 and 115 Ma, similar to fossil ages (Cumming and Kesler, 1987). The Pueblo Viejo Maar-Diatreme Mb hosts one of the largest gold–silver deposits in the world (Kesler et al., 2003). Recently, Nelson (2000) re-defined the stratigraphy of the LRF at Pueblo Viejo mine district and suggested that volcanism, dome emplacement, erosion and epiclasts accumulation, hydrothermal alteration and gold mineralization were coeval Early Cretaceous events. The Hatillo Fm, a massive reef limestone of Albian age, rest unconformably on LRF.

4. Geology of the Los Ranchos Fm

The LRF comprises a >3-km-thick sequence of volcanic and volcaniclastic rocks with variable geochemical characteristics, which is intruded by tonalite batholiths, minor diorite to gabbro plutons, and mafic dykes. Three cartographic units have been defined in the LRF at the Cevicos-Miches area of the Cordillera Oriental (Figs. 2 and 3).

The lower basaltic unit is dominated by spilitized polymict volcanic breccias and flows of boninite,

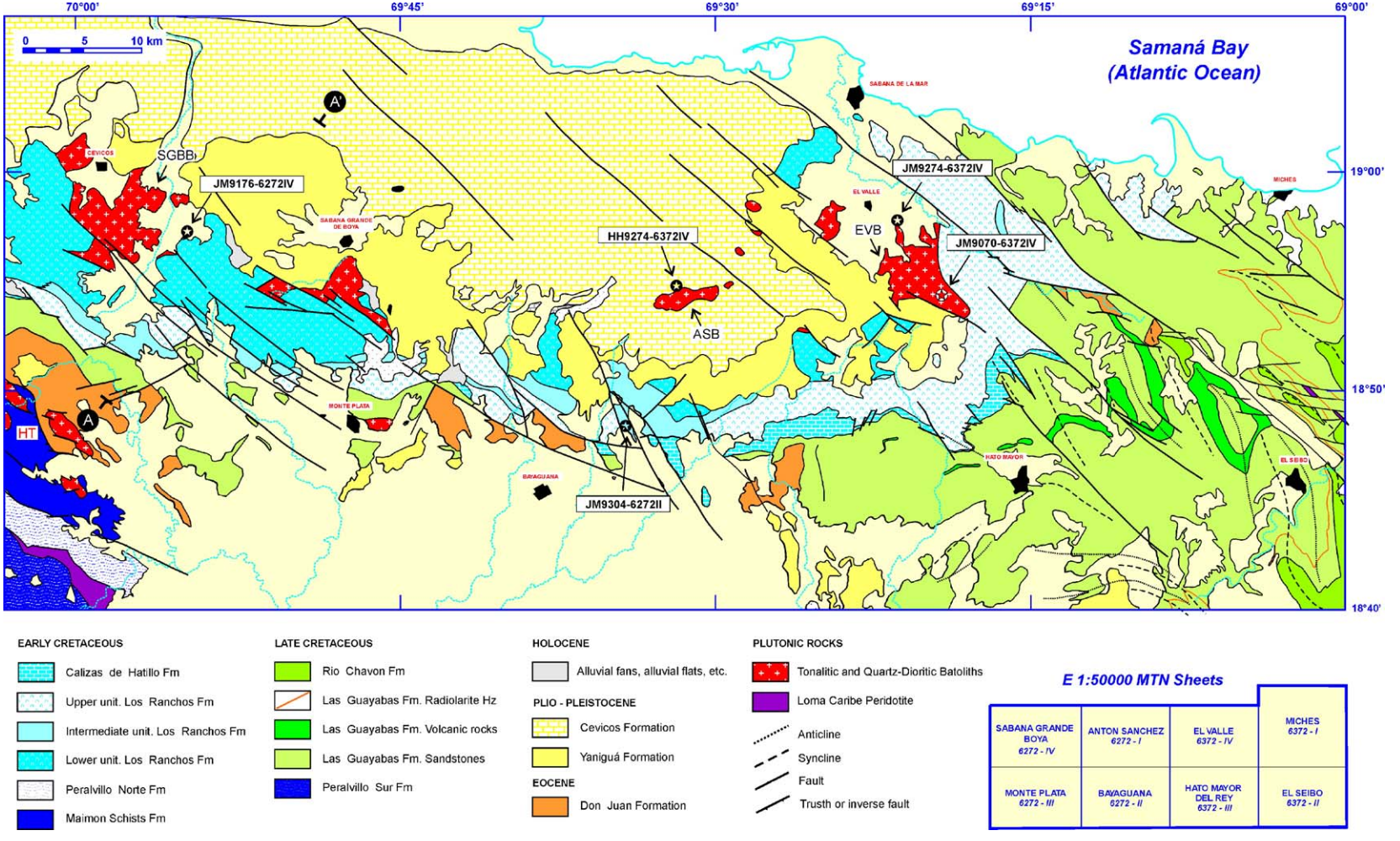

Fig. 2. Geological map of the Cordillera Oriental, Dominican Republic (SYSMIN Project). Coordinates are UTM values from 1 : 50,000 National Topographic Map. A–A′ is the cross-section of Fig. 3.

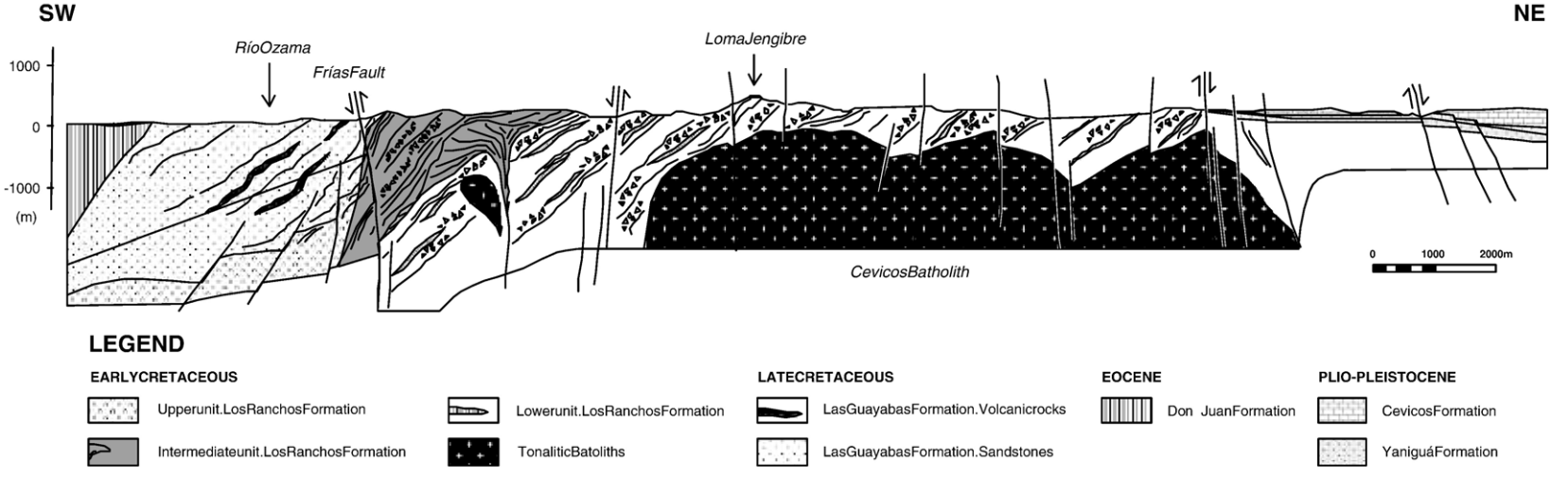

Fig. 3. Geologic cross-section through the W Cordillera Oriental showing the stratigraphic relations in the Los Ranchos Fm.

boninitic and tholeiitic basalt to basaltic andesite, with local pillow lavas and interbedded well-stratified, fine-grained volcaniclastic rocks. Both the basalts and andesites are present throughout the volcanic stratigraphy, although the basaltic rocks are most prevalent at the base of the exposed sequence. The volcanic rocks of the lower LRF erupted in a submarine environment and are intruded by syn-volcanic dykes and sills of microgabbro. Coarse- to medium-grained volcaniclastics occur locally in the upper part of the lower unit. In other places, upward-fining volcaniclastic sequences of spilitized tuffs and sandstones also occur. This unit mainly crop out in the Sabana Grande de Boyá and El Valle E. 1:50,000 sheets (Fig. 2), with a thickness of more than 1500 m and is intruded at its base by tonalitic batholiths. The basalts are light to dark green and texturally range from porphyritic (predominantly) to vesicular/amygdaloidal and aphyric. They contain orthopyroxene, clinopyroxene and plagioclase phenocrysts, with fibrous antigorite pseudomorphs after olivine, rarely fresh. Andesites are characterized by glomeroporphyritic aggregates of pyroxene, plagioclase and iron oxide. Plagioclase is the most abundant phenocryst phase (<35% modal) and roughly equal proportions of euhedral or subhedral ortho- and clinopyroxene.

The intermediate rhyodacitic unit (Fig. 3) is componed by altered dacite to rhyolite flows, brecciated extrusive domes and criptodomes, with minor intermediate to felsic monogenetic silicified tuffs, crystal-rich tuffs, lapilli tuffs and packets of upward-fining volcaniclastic sandstones to siltstones. Characteristically, dacites and rhyolites are beige-yellow and pink to greenish gray and porphyritic, with abundant feldspar and quartz phenocrysts. These rocks were erupted as shallow submarine flows and pyroclastic deposits produced by phreatomagmatic explosions, with local subvolcanic intrusions. In this unit there are small sulphide deposits associated with the rhyolites and interpreted as the stockwork alteration zone of volcanogenic massive sulphide deposits. The unit has a thickness of about 500–1000 m in the Sabana Grande, Antón Sanchez and Bayaguana sheets and pinches out to the E in the Hato Mayor and El Valle sheets areas.

The upper basaltic unit is about 1000 m thick and composed of dark green to black altered tholeiitic basalt to andesite, forming massive flows, autoclastic breccias and syn-volcanic gabbroic intrusions. The coherent rocks are ortho- and clinopyroxene-bearing porphyritic basalts and plagioclase-phyric basalts, with minor olivine and clinopyroxene-bearing basalts. Textures are locally vesicular/amygdaloidal and autoclastic breccias are generally composed by monogenetic clasts. Thick sequences of massive flows of porphyritic basalts occur in the Bayaguana (Pan de Azúcar) and Hato Mayor areas, where microgabbros and dolerites are interpreted as the internal part of lobes and feeder dykes. These volcaniclastic deposits grade to an upper sequence of lithic tuffs, volcanic sandstone and fossiliferous sediments. The basal part of the unit was deposited as submarine debris flows and mass flows and the upper part as sedimentary rocks with significant volcanic debris. In the Antón Sánchez area, the upper basaltic unit is locally overlain by 50–100 m of vesicular dacitic to rhyolitic lavas and lava breccias, with related syn-volcanic intrusions of rhyolitic domes. Felsic flows are dominantly porphyritic, with quartz and feldspar phenocrysts over reddish to brown aphanitic devitrified matrix. The felsic volcanic rocks are locally interbedded with lapilli tuffs and volcanic-derived fine-grained clastic sedimentary rocks. At the top of the sequence, unconformably bellow the Hatillo Fm, a thin sequence of basaltic to andesitic lavas locally occurs.

The LRF is intruded by Sabana Grande, Antón Sanchez and El Valle tonalite batholiths (Fig. 2), gabbroic to dioritic individual plutons or minor rim facies, and a set of mafic to intermediate dykes. Tonalitic batholiths generally lack any macroscopic deformation. The main recognized petrographic types are coarse- to medium-grained isotropic hornblende±biotite tonalite; fine-grained clinopyroxene–hornblende diorite, and fine-grained hornblende quartz–diorite. Locally, the tonalite contains a large proportion of elongate parallel hornblende diorite inclusions, which probably represent dismembered dykes or the product of magma mixing. A set of mafic to intermediate dykes crosscut tonalites and hornblende diorite. Several petrographic types of dykes were recognized, including the following: fine-grained to aphanitic dark grey microgabbro, dark subophitic microgabbro, fine-grained light grey dolerite, and aphanitic, dark green, sparsely phyric dolerite. Fragments of both hornblende diorite and dykes occur in the tonalite. Geochemically similar rock types (see bellow) also occur as irregular sectors or intrusions within the diorite and gabbro rim facies and altered pods within the tonalite batholiths. These probably represent either inclusions that have resided in the tonalite for extended periods of time and have lost their coherence, or the product of magma mixing.

5. Geochronology

The U–Pb and $^{40}Ar/^{39}Ar$ ages for felsic volcanic rocks of LRF and intrusives are presented below. The geological map of Fig. 2 indicates the sample locations.

Analytical procedures are in Appendix 1. All ages are quoted at the 2σ level of uncertainty.

5.1. U–Pb samples

A porphyritic dacite from the felsic flows/domes of the intermediate rhyodacitic unit in the Bayaguana sheet (sample JM9304-6272-II) and an unfoliated tonalite from the Zambrana stock located in the Hatillo sheet (sample 95101-6172-IV) were dated. The Zambrana stock intrudes the lowest stratigraphic level of the LRF, which is the Cotui and Quita Sueño Mb in this area (Kesler et al., 1990). Mafic dykes, which crosscut volcanic rocks of the LRF, did not yield any datable minerals. The porphyritic dacite age was determined from five abraded zircon fractions. Zircon grains are clear to slightly cloudy, pale yellow, euhedral prisms, with aspect ratios of ~1.5–3.5. Three fractions (B, D and E) are concordant (Fig. 4a) and give an age of 116.0±0.8 Ma (Appendix 2). This Aptian (geologic time scale from Gradstein et al., 2004) age is interpreted as the crystallization age of the sample. The age of the tonalite was determined from three strongly abraded zircon fractions. All yielded concordant analyses (Fig. 4b). Fraction B gives the oldest $^{206}Pb/^{238}U$ age, at 115.5± 0.3 Ma. This Aptian age is interpreted as the crystallization age of the sample and lies within error of the dacite age. The similarity in

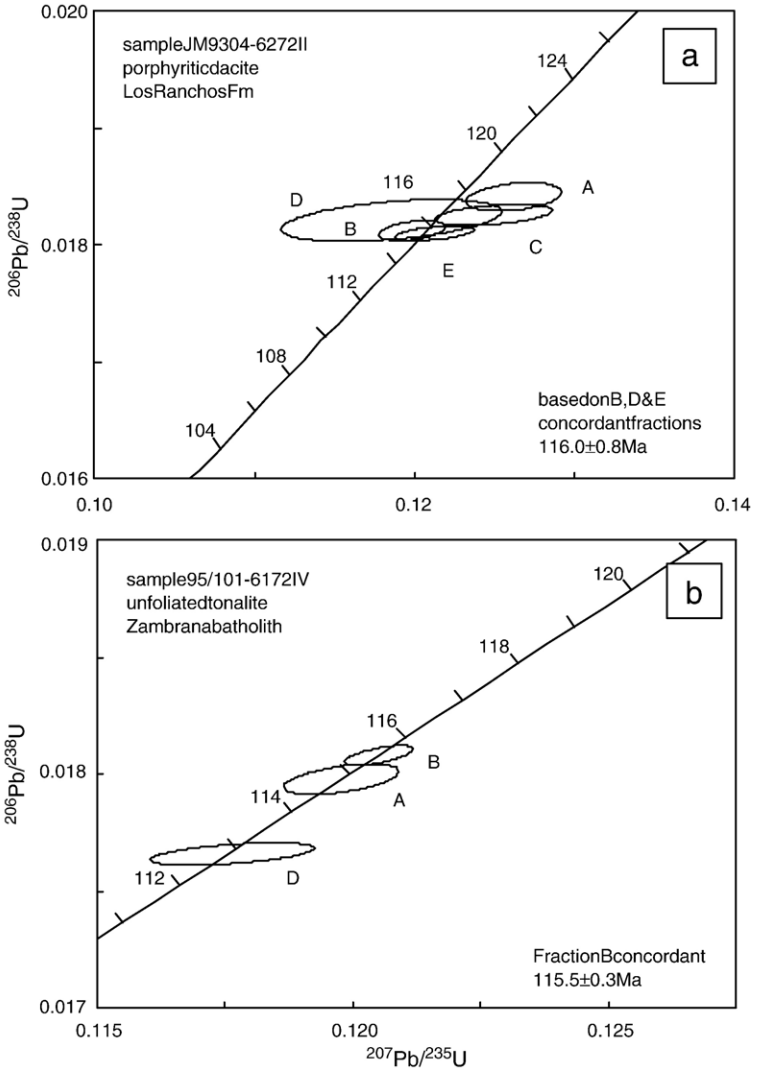

Fig. 4. Concordia diagrams for (a) porphyritic dacite from the felsic flows/domes of the intermediate rhyodacitic unit in the Bayaguana sheet area (JM9304-6272-II) and (b) unfoliated tonalite from the Zambrana stock located in the Hatillo sheet area (95101-6172-IV). See text for discussion. U–Pb analytical data are in Appendix 2.

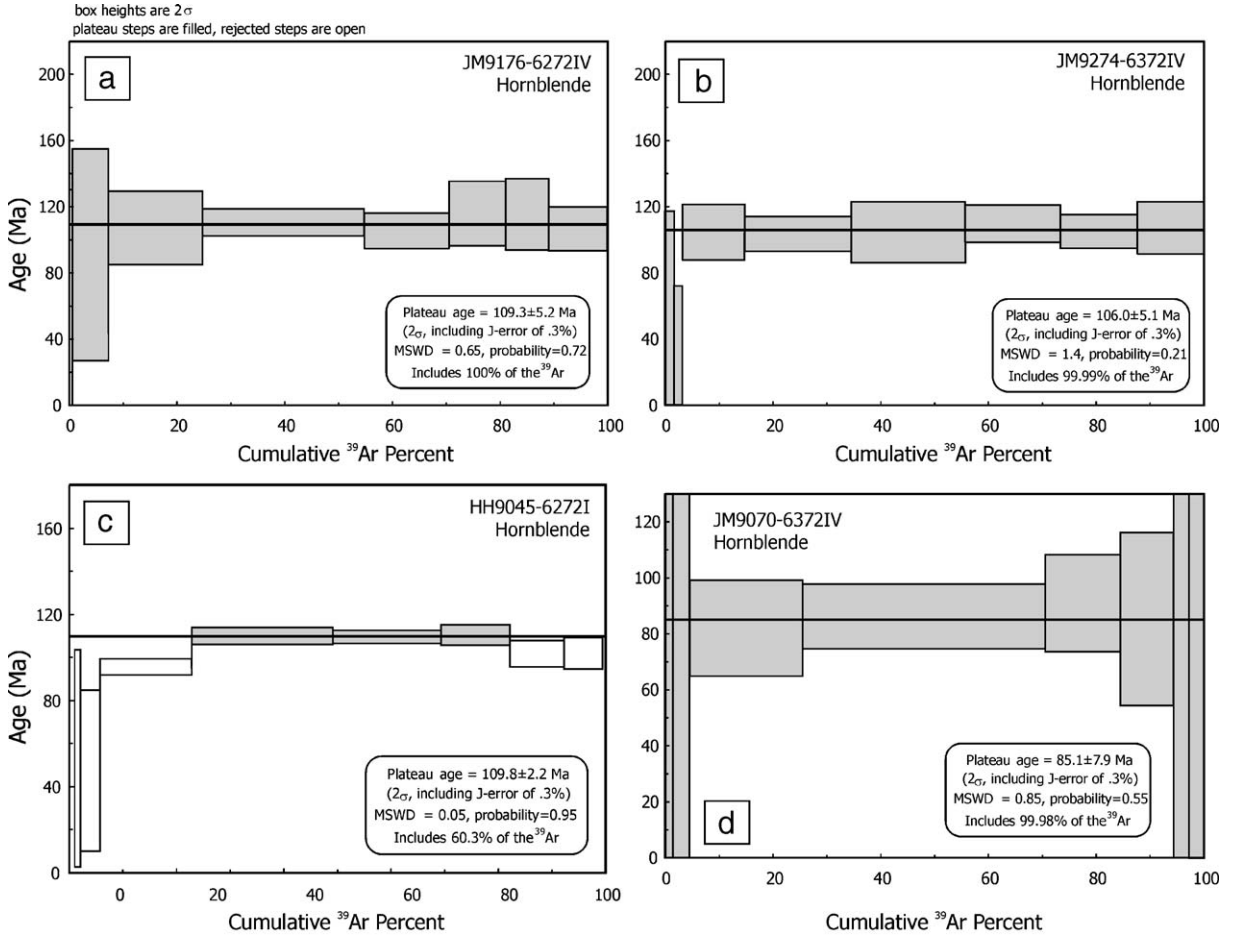

Fig. 5. $^{40}Ar/^{39}Ar$ age spectra for hornblende in tonalite and mafic dyke from the Cevicos, Sabana Grande de Boyá and El Valle batholiths. The plateau ages were calculated following techniques described in Appendix 1. A summary of ^{40}Ar–^{39}Ar incremental heating experiments is in Appendix 3. Errors are quoted at the 2σ (95% confidence) level and are propagated from all sources except mass spectrometer sensitivity and age of the flux monitor. See text for discussion.

ages and geochemistry (see below) implies a genetic link between felsic volcanic rocks of LRF and the voluminous tonalite magmatism.

5.2. $^{40}Ar/^{39}Ar$ samples

Hornblende-bearing granitoids and related mafic dykes of the Cevicos, Sabana Grande de Boyá and El Valle batholiths were selected for $^{40}Ar/^{39}Ar$ dating (Fig. 5a–d; Appendix 3). Sample JM9176-6272IV is a coarse- to medium-grained isotropic hornblende quartz-diorite from the rim facies of the Cevicos batholith (Sabana Grande de Boyá). For all steps (1–8), the obtained plateau age from hornblende is 109.3±5.2 Ma (MSWD=0.65) for 100% of the ^{39}Ar released. Sample JM9274-6372IV is a fine-grained microgabbro that crosscuts the hornblende±biotite tonalite facies of the El Valle batholith (El Valle). This sample yielded a plateau age for hornblende of 106.0±5.1 Ma (MSWD=1.4) for all steps (1–8) and 99.99% of the ^{39}Ar released. Sample HH9045-6272I is a coarse- to medium-grained hornblende tonalite from the outcrop isolated by the Haitises limestones (Antón Sánchez). The plateau age for hornblende is 109.8±2.2 Ma (MSWD=0.053) for the high-temperature 4–6 steps and 60.3% of the ^{39}Ar released. Sample JM9070-6372IV is a coarse-grained subequigranular isotropic hornblende±biotite tonalite, which constitute the facies of El Valle batholith. The obtained hornblende plateau age is 85.1±7.9 Ma (MSWD=0.85) for all steps (1–8) and 99.98% of the ^{39}Ar released.

5.3. Interpretation

In the area south of Cotui, U/Pb age of 115±0.3 Ma for the Zambrana tonalite and 116.0±0.8 Ma for a dacite of the intermediate unit of the LRF overlap within analytical error, suggesting contemporaneous formation of both units during the Aptian. Similarly, $^{40}Ar/^{39}Ar$ ages of hornblende from the Cevicos, Sabana Grande and Antón Sanchez tonalite batholiths, and microgabbro dykes from El Valle batholith, overlap within analytical uncertainties (108.3±4.1 Ma) and are interpreted as Albian cooling ages after emplacement of these intrusions. Further, microgabbro dykes cuts hornblende-bearing tonalites in the El Valle batholith, and the tonalite locally contains a large proportion of microgabbroic and hornblende–diorite inclusions, which suggest that mafic and felsic magmatism have occurred, in part, synchronously. Geochemical characteristics outlined below suggest that the dated microgabbro is geochemically related to mafic volcanic rocks and hornblende tonalites are the intrusive equivalents to felsic volcanic rocks of the LRF. A tonalite from the El Valle batholith (JM9070) yielded an imprecise but young Ar–Ar age of 85.1±7.9 Ma, similar to the whole rock 95±4.8 and 87.3±4.4 Ma ages obtained by the K–Ar method in the same tonalitic massif by Bourdon (1985). These ages are, however, inconsistent with the Albian age of the Hatillo Limestone (112–100 Ma), which lies unconformably on top of the El Valle batholith. Probably, the Coniacian–Santonian age reflect a local thermal resetting induced by the Upper Cretaceous magmatism and related hydrothermal fluid activity.

6. Geochemistry

6.1. Alteration and metamorphism

In the previous sections, data were presented to show that felsic volcanic rocks of the LRF and the tonalitic magmatism are spatial and temporary linked, and the microgabbro dykes and mafic volcanics are in part synchronous. The objectives of this section are to show that there is petrogenetic relationship between these groups of rocks, to distinguish different geochemical mafic volcanic groups, and to interpret the tectonic setting in which they formed. Geochemical data are reported in Table 1. A representative suite of samples of LRF was also analysed for Rb–Sr and Sm–Nd isotopic compositions (Table 2). Details of analytical techniques are in Appendix 1.

However, before making petrogenetic interpretations based on bulk-rock geochemistry, the mobility of the elements must be evaluated. Rock samples of the LRF have been variably metamorphosed to prenhite-pumpellite and lower greenschist facies, and many of the volcanic rocks have spilitic mineral assemblages typical of seafloor alteration, although igneous textures and pyroxene phenocrysts can still be recognized. Many major (e.g., Si, Na, K, Ca) and trace (e.g., Cs, Rb, Ba, Sr) elements are easily mobilised by late and/or post-magmatic fluids and under metamorphism; however, the HFSE (Y, Zr, Hf, Ti, Nb and Ta), rare earth elements (REE), transition elements (V, Cr, Ni and Sc) and Th, may be relatively immobile under a wide range of metamorphic conditions (Pearce, 1983; Bienvenu et al., 1990), including seafloor alteration at low to moderate water/rock ratios. In a K_2O+Na_2O vs. $K_2O/(K_2O+Na_2O)$ plot (not show), which may be used to screen samples for spilitization and K-metasomatism, the sampled plutonic rocks and mafic dykes plot in or near the igneous spectrum suggest that even these easily

Table 1
Whole-rock geochemical data for Los Ranchos Formation

Type	I							II			
Sheet	6372-III	6272-I	6372-IV	6372-IV	6372-III	6372-I	6372-IV	6272-I	6272-II	6272-IV	6272-IV
Unit	Upper	Upper	Upper	Upper	Upper	Intermediate	Upper	Lower	Lower	Lower	Lower
Rock	Mflow	Ituff	Iflow	Mflow	dyke	dyke	Mgab	Mflow	Mflow	Gab	Mtuff
Sample	JG9074	HH9038	JM9158	JM9636	JG9072	AD9037	JM9274	HH9035	JM9320	JM9177	JM9289
SiO_2	48.86	61.04	57.23	53.52	48.49	54.81	49.79	54.17	53.8	52.49	52.3
TiO_2	0.92	0.68	0.95	0.98	0.94	0.78	1.01	0.79	0.67	0.63	0.53
Al_2O_3	19.29	16.05	15.51	17.3	19.6	15.63	16.43	17.6	17.66	16.76	16.61
Fe_2O_3	9.52	6.9	9.32	9.34	9.31	8.85	10.67	10	8.34	10.77	10.58
MgO	3.17	2.72	3.21	3.95	3.97	4.41	6.21	3.91	3.56	4.64	4.71
CaO	9.4	4.89	3.79	8.17	10.89	5.79	10.75	9.29	9.05	8.53	9
Na_2O	3.01	3.76	6.05	3.44	2.71	2.69	2.54	2.02	2.34	2.52	3.89
K_2O	0.58	0.24	0.11	0.31	0.3	1.72	0.18	0.19	0.5	0.33	0.36
P_2O_5	0.08	0.12	0.11	0.13	0.1	0.27	0.08	0.07	0.09	0.04	0.01
MnO	0.12	0.24	0.19	0.16	0.14	0.2	0.16	0.16	0.14	0.17	0.2
Cr_2O_3	0.003	0.009	0.0005	0.005	0.007	0.023	0.015	0.015	0.018	0.018	0.008
LOI	4.3	3	3.1	2.4	3	4.6	1.8	1.4	3.4	2.4	1.3
SUM	99.29	99.68	99.6505	99.795	99.47	99.91	99.745	99.64	99.58	99.32	99.52
Mg#	39.74	43.84	40.55	45.58	45.78	49.67	53.54	43.64	45.81	46.04	46.85
Ni	12.3	3.9	10.2	Nm	12.6	68.2	34.2	7.3	9.1	14.4	9.6
Co	31.6	14	18.4	21.8	27.9	45.4	36.4	26	23.6	31.7	34.8
Sc	34	26	39	35	38	25	46	41	35	44	46
V	301	132	170	239	316	231	319	289	246	328	283
Rb	8.9	3.1	1	3	2	27.4	3.8	1.3	6.8	1	2.2
Ba	248	206	30	143	79	1122	107	139	117	62	70
W	0.4	1.2	0.8	0.7	0.5	2.3	1.8	2.3	2	2.9	0.6
Th	0.1	0.5	0.3	0.4	0.4	1.8	0.4	0.3	0.2	<.1	<.1
U	<1	0.3	0.1	0.2	<.1	0.7	0.1	<.1	<.1	0.1	<.1
Nb	0.2	0.9	0.8	1.2	0.5	2.1	1.2	0.6	0.8	0.2	0.7
La	2	5.5	3.1	3.7	2.1	17.4	3.4	1.3	2.1	0.7	0.6
Ce	6.1	11.5	8.6	10.2	5.6	33.4	8.7	3.8	5.7	2.7	2.1
Pb	0.5	1.6	1	1.2	0.4	5.5	0.3	0.3	1	0.3	0.2
Pr	0.93	2.05	1.5	1.76	0.92	4.38	1.36	0.72	0.92	0.46	0.4
Mo	0.3	1.2	0.7	0.6	0.3	1.3	1	1.7	2.1	2.1	0.6
Sr	1527	240	70	280	498	393	237	174	606	121	138
Nd	5.3	12.5	9.3	10.2	5.4	23.1	8.5	5.1	6.4	3.2	2.7
Sm	2.1	3.7	3.4	3.4	1.8	6.2	2.4	1.7	2.1	1.3	1.2
Zr	33.8	49.8	55.3	64.3	30.3	45.3	49.5	21.6	35	20	17.6
Hf	1.1	1.7	2.1	2.4	1.2	1.6	1.6	0.8	1.3	0.6	0.6
Eu	0.87	1.15	1.11	1.12	0.81	2.28	0.88	0.74	0.7	0.56	0.5
Gd	2.87	4.47	4.18	4.21	2.57	7.76	2.95	2.39	2.92	1.99	1.82
Tb	0.59	0.79	0.75	0.82	0.53	1.5	0.54	0.51	0.53	0.33	0.35
Dy	3.52	4.37	4.93	5	3.08	8.15	3.15	2.97	3.72	2.66	2.22
Y	23.2	28.7	31.8	31.1	19	42.1	20.4	17	21.2	15.6	14.6
Ho	0.78	0.95	1.08	0.98	0.65	1.74	0.69	0.7	0.76	0.54	0.48
Er	2.36	2.75	3.19	3.02	2.01	5.18	1.99	1.97	2.24	1.67	1.5
Tm	0.3	0.41	0.48	0.46	0.31	0.79	0.32	0.28	0.38	0.25	0.22
Yb	2.25	2.34	3.1	2.87	1.9	4.93	1.89	1.72	2.17	1.96	1.55
Lu	0.38	0.4	0.49	0.47	0.32	0.81	0.28	0.27	0.33	0.31	0.23
$(Zr/Sm)_N$	0.64	0.53	0.64	0.75	0.67	0.29	0.82	0.50	0.66	0.61	0.58
$(La/Yb)_N$	0.64	1.69	0.72	0.93	0.79	2.53	1.29	0.54	0.69	0.26	0.28

Total Fe as Fe_2O_3. For calculating Mg# $FeO = 0.8 \times Fe_2O_3$ total and $Fe_2O_3 = 0.2 \times Fe_2O_3$ total.Rock type: Mflow=mafic flow; Iflow=intermediate flow; Mtuff=mafic tuff; Ituff=intermediate tuff; Ftuff=felsic tuff; dyke=late dyke; Mvolc=mafic volcanic; Ivolc=intermediate volcanic; Fvolc=felsic volcanic; Mgab=microgabbro; gab=massive gabbro; Rhy=rhyolite; Rhydc=rhyodacite; Tnl=tonalite; Qdio=quartz–diorite; SGB=Sabana Grande batholith; CB=Cevicos batholith; ASB=Antón Sánchez batholith; EVB=El Valle batholith. See Appendix 1 for analytical details.

				III			IV				
6272-IV	6272-I	6372-I	6272-IV	6372-I	6272-IV	6172-IV	6272-I	6272-II	6272-I	6272-II	6272-IV
Lower	Lower	Lower	Lower	Lower	Lower	Lower	Interm	Interm	Upper	Interm	Interm
Mflow	Mflow	Mflow	Mflow	Iflow	Mvolc	Iflow	Rhy	Rhy	Rhy	Rhy	Fvolc
JM9598	HH9019	AD9035	JM9022	AD9034	02J100	02J102	HH9046	JM9304	HH9071	JM9365	JM9600
49.27	48.2	48.91	43.49	56.25	52.9	53.07	82.14	78.18	72.57	76.72	76.34
0.72	0.74	0.39	0.46	0.48	0.17	0.18	0.18	0.18	0.49	0.32	0.26
16.91	18.06	14.21	13.73	15.91	12.44	15.4	9.97	11.48	13.54	11.59	12.02
9.99	9.93	8.3	7.61	8.31	6.47	8.24	1.18	1.42	3.7	2.1	3.23
5.65	6.49	6.52	7.37	4.88	7.26	7.52	0.07	0.16	0.48	0.35	0.55
9.06	9.02	9.8	14.95	5.35	9.08	7.44	0.25	0.29	0.63	0.8	0.47
3.5	2.7	3.09	2.07	5.64	5.17	5.3	4.91	3.4	5.58	4.01	5.84
0.29	0.15	0.49	0.19	0.15	0.36	0.16	0.05	3.53	1.34	2.55	0.03
0.04	0.11	0.05	0.05	0.03	0.02	0.01	0.005	0.01	0.09	0.04	0.04
0.16	0.15	0.14	0.22	0.14	0.16	0.19	0.01	0.03	0.04	0.03	0.07
0.007	0.009	0.05	0.065	0.032	0.051	0.075	0.019	0.024	0.028	0.028	0.058
4	4.2	7.8	9.3	2.8	5.6	3.02	1.1	0.8	1.5	1.2	0.8
99.61	99.78	99.78	99.53	99.98	99.7	100.6	99.89	99.524	100.04	99.808	99.72
52.83	56.41	60.87	65.73	53.77	68.96	60.33	10.51	18.24	20.44	24.82	25.22
11.3	23.6	112	86	45.3	36.3	107	5.8	7.2	8.5	12.6	14.8
39.7	36.1	37.3	36.9	27.6	31	34	2.3	0.9	5.3	3.9	3.4
42	41	35	37	37	38	52	5	8	17	9	13
345	327	255	260	258	153	268	20	17	18	21	7
2.3	1.4	6.8	1.1	1.4	5.1	5.2	<0.5	35.9	10.8	21.8	<0.5
61	77	130	37	44	46	36	31	1576	373	355	20
0.7	0.6	0.4	1.7	2.1	<.1	1.8	4.3	5.2	5.7	6.9	14.6
0.1	0.3	0.1	<.1	0.2	<.1	0.12	0.5	0.9	1.2	1.6	0.4
0.1	<.1	1.5	0.2	0.2	0.1	0.4	0.4	0.5	0.4	0.7	0.2
0.8	0.8	1	0.7	2.1	0.3	0.5	1	1	1.7	2.7	1.7
2.2	2.2	1.1	1.4	1.3	0.6	0.54	4.2	13.4	5.7	8.6	3.8
2.9	5.9	2.7	2.8	2.9	1	1.2	8.9	18.1	15.3	22.2	12.9
0.2	0.4	0.8	0.5	1.2	0.2	1.8	0.9	1.2	2.8	1.1	0.6
0.55	0.92	0.4	0.58	0.51	0.2	0.17	1.88	4.12	2.07	3.42	2.15
0.5	0.4	0.3	0.6	1.6	0.3	–	3.1	3	2.8	4.9	9.9
223	316	141	173	74	115	102	33	117	135	70	33
3.2	6.4	2.5	3.3	2.8	1.1	0.8	10	20.4	12.6	17.4	11.9
1.4	1.7	1.1	1.4	1	0.5	0.32	3.2	5.6	3.2	5	4.3
19.2	22.3	20.5	18.2	26	13.1	10	78.6	95.6	105.5	189.6	110.4
0.7	0.9	1.1	0.7	0.9	<.5	0.3	2.9	3.3	3.9	6.2	4
0.62	0.63	0.37	0.49	0.41	0.19	0.12	0.78	1.25	0.81	0.87	0.95
1.93	1.87	1.55	2.11	1.56	0.56	1.24	2.52	6.97	4.17	5.88	6.19
0.35	0.42	0.34	0.36	0.35	0.11	0.08	0.47	1.32	0.78	1.15	1.15
2.51	1.93	1.77	2.22	2.4	0.64	0.57	2.95	8.07	4.44	7.39	7.37
13.8	12	11	14.5	14.6	3.6	3.2	12.8	60.6	30.3	50	45.9
0.52	0.46	0.4	0.51	0.53	0.13	0.13	0.53	1.76	1.03	1.64	1.67
1.76	1.3	1.24	1.54	1.66	0.36	0.45	1.64	5	3.42	5.09	5.27
0.22	0.2	0.22	0.28	0.27	0.06	0.07	0.24	0.72	0.5	0.74	0.82
1.61	1.16	1.19	1.62	1.86	0.65	0.5	1.85	5.01	3.37	5.29	5.39
0.24	0.17	0.23	0.24	0.27	0.09	0.08	0.31	0.84	0.54	0.88	0.86
0.54	0.52	0.74	0.52	1.03	1.04	1.24	0.97	0.68	1.31	1.50	1.02

(continued on next page)

Table 1 (*continued*)

Type	IV				Batho			
Sheet	6372-III	6272-I	6272-I	6173-II	6272-IV	6272-IV	6272-I	6372-IV
Unit	Interm	upper	Interm	Lower	SGB	CB	ASB	EVB
Rock	Ftuff	Rhydc	Rhy	Rhy	Tnl	Qdio	Tnl	Tnl
Sample	JG9068	HH9072	HH9049	02J124	JM9181	JM9176	HH9044	JM9070
Al_2O_3	13.19	14.91	11.86	12.43	12.85	13.42	13.38	14.4
Fe_2O_3	4.18	2.85	3.05	2.6	3.27	4.73	3.25	4.77
MgO	0.75	0.55	0.63	1.81	0.65	1.21	0.86	1.37
CaO	0.27	1.18	1.58	0.27	2.4	4.17	3.33	3.68
Na_2O	6.1	5.68	3.57	5.04	4.35	3.47	4.13	4.33
K_2O	0.55	1.1	1.21	0.49	0.76	0.5	0.47	0.92
P_2O_5	0.08	0.11	0.03	0.08	0.06	0.03	0.08	0.09
MnO	0.13	0.03	0.04	0.06	0.06	0.1	0.05	0.1
Cr_2O_3	0.007	0.013	0.027	0.012	0.028	0.025	0.022	0.03
LOI	1.6	2.1	2.2	2	1	1.3	1	1.4
SUM	99.89	100.08	99.98	99.77	100.15	99.79	99.79	99.78
Mg#	26.22	27.65	29.03	57.96	28.25	33.63	34.38	36.26
Ni	2.2	8.5	6.2	3.9	5.2	9.6	4.3	12.8
Co	1.5	5.8	5	4.5	3.4	7	4	8.2
Sc	17	19	10	7	13	18	16	14
V	7	24	22	36	16	67	37	62
Rb	9.8	14.8	22.1	8.5	12.7	3.2	9.9	12.2
Ba	133	304	213	42	217	212	171	202
W	1.4	2.7	5.7	3.8	5.9	5.1	5.4	6.7
Th	0.4	0.9	2	1	0.5	0.6	0.4	0.9
U	0.1	0.9	0.6	0.5	0.3	0.2	0.3	0.4
Nb	2.7	2.4	2.8	1.4	1.4	1.2	1.8	1.9
La	5.9	6	8.7	11.5	4.3	2.7	3.7	8.1
Ce	14.9	14.9	23.5	24	13.6	8.4	11.8	22
Pb	1.6	2.1	0.6	20.9	0.4	0.4	0.4	0.3
Pr	2.31	2.38	3.65	3.14	2.43	1.42	2.16	3.35
Mo	1.1	1.7	3.6	2.8	4.4	3.7	3.8	5.6
Sr	45	295	78	24	75	77	98	143
Nd	12.4	11.7	18.6	15.4	14.3	8	13.8	17.5
Sm	4	4.1	5.3	3.7	5.2	3.4	4.4	4.6
Zr	170.3	119.1	182.9	119.9	112	88.2	114.5	138.4
Hf	5.1	3.9	6	3.9	4.2	3.1	4.2	4.6
Eu	1.34	1.12	0.87	0.87	0.9	0.8	1.26	1.21
Gd	5.38	4.97	5.77	3.73	6.56	5.05	6.29	5.21
Tb	1.1	0.94	1.17	0.7	1.33	0.95	1.2	1.02
Dy	7.33	5.78	7.14	4.64	8.3	6.63	7.58	6.34
Y	50.2	35.9	46.4	28.7	57.3	44.1	48.9	43.3
Ho	1.74	1.32	1.67	1	1.87	1.44	1.67	1.41
Er	5.67	3.77	5.16	3.09	5.67	4.55	5.3	4.34
Tm	0.84	0.58	0.77	0.45	0.92	0.65	0.78	0.65
Yb	6	3.77	5.62	3.08	6.13	4.65	4.8	4.18
Lu	0.98	0.61	0.86	0.54	0.97	0.76	0.77	0.73
$(Zr/Sm)_N$	1.69	1.15	1.37	1.28	0.85	1.03	1.03	1.19
$(La/Yb)_N$	0.71	1.14	1.11	2.68	0.50	0.42	0.55	1.39

Table 2
Sr–Nd isotope ratios for representative rocks of the Los Ranchos Formation

Unit	Rock	Type	Sample	$^{87}Sr/^{86}Sr$	$(^{87}Sr/^{86}Sr)_i$	$(\varepsilon_{Sr})_i$	$^{143}Nd/^{144}Nd$	$(^{143}Nd/^{144}Nd)_i$	$(\varepsilon_{Nd})_i$
LRF	Andesitic basalt	I	JG9067	0.704305 (6)	0.704296	−0.99	0.513157 (12)	0.513005	10.06
LRF	Andesitic basalt	I	JM9636	0.703383 (12)	0.703332	−14.68	0.513150 (26)	0.512998	9.92
LRF	Basalt	II	JM9022	0.704617 (9)	0.704586	3.13	0.513128 (8)	0.512935	8.68
LRF	Andesitic basalt	II	JM9289	0.705759 (7)	0.705683	18.70	0.513144 (6)	0.512941	8.82
LRF	Gabbro	II	JM9177	0.704455 (6)	0.704415	0.70	0.513161 (8)	0.512976	9.49
LRF	Basalt (lava)	III	AD9035	0.70557 (8)	0.705342	13.85	0.513101 (10)	0.512900	8.02
LRF	Basalt	III	02J100	0.70552 (6)	0.705292	13.14	0.513132 (8)	0.512938	8.74
LRF	Riolite	IV	JM9304	0.705624 (8)	0.704169	−2.80	0.513089 (6)	0.512964	9.25
LRF	Microgabbro	IV	JM9274	0.703042 (6)	0.702966	−19.88	0.513107 (6)	0.512978	9.53
LRF	Rhyolite	IV	HH9044	0.704305 (7)	0.703828	−7.64	0.513130 (10)	0.512984	9.66
LRF	Tonalite	Batholith	JM9176	0.704282 (8)	0.704084	−4.01	0.513155 (6)	0.512961	9.20
LRF	Tonalite	Batholith	JM9070	0.703522 (6)	0.703119	−17.70	0.513090 (5)	0.512970	9.37

Unit: LRF=Los Ranchos Fm. Calculated initial ratios (i) and ε_{Sr} and ε_{Nd} values calculated at t=115 Ma. Number in parentheses is the absolute 2σ error in the last decimal places. ε_{Nd} values are relative to $^{143}Nd/^{144}Nd$=0.512638 and $^{147}Sm/^{144}Nd$=0.1966 for present day CHUR and lambda $^{147}Sm=6.54\times10^{-12}$/year. See Appendix 1 for analytical details.

mobilized elements have not been significantly changed by metamorphism. But most of the volcanic rocks of the LRF plot are in the spilitized field. However, studies of altered seafloor basalts (e.g., Humphris and Thompson, 1978) suggest that the major element ratio MgO/FeO is not significantly changed by spilitization, and thus reflects igneous processes. On extended REE plots (see below), dykes and related volcanic rocks show little variation in their patterns, and thus the above-mentioned trace elements are believed to have retained their igneous relative abundances despite spilitization. In the discussion on the petrogenesis and tectonic setting of the mafic volcanic suites within LRF bellow, it is assumed that the REE and HFS elements, as well as the Sm–Nd isotopic system, were not significantly affected by secondary alteration at the whole-rock scale.

6.2. Geochemical characteristics of mafic rocks

The geochemical characterization of mafic rocks of LRF is based in samples interpreted to best represent liquid compositions, although partially cumulate massive gabbros were also included for comparison. The syn-volcanic microgabbro or dolerite dykes, aphyric flows and pillowed basalts provide the best estimates of liquid compositions as they do not commonly contain abundant phenocrysts. 30-cm-size, homogeneous

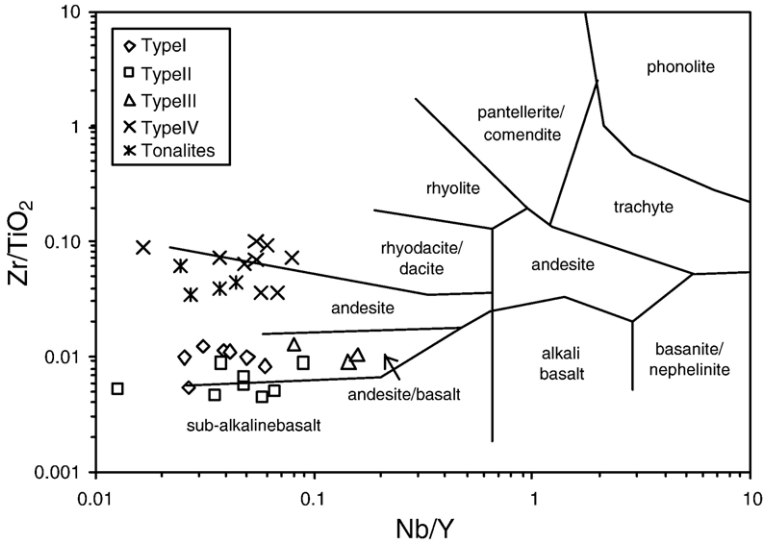

Fig. 6. Nb/Y vs. Zr/TiO_2 diagram (Winchester and Floyd, 1977) for mafic and felsic volcanic rocks of the Los Ranchos Fm and tonalite batholiths.

aphyric clasts of basalt in volcanic breccias are also interpreted represent a liquid composition. Petrographic observations suggest that the microgabbro (JM9274) and hornblende gabbro/diorite (JM9177) from El Valle and Sabana Grande batholiths, respectively, does not have a significant cumulate component and may also provide a good indication of liquid compositions. Gabbros have very similar trace element patterns to the mafic dykes and volcanic rocks, suggesting that the possible accumulated minerals have preserved the relative trace element abundances characteristic of the magmas from which they were derived. Primitive mantle-normalized, extended REE diagrams provide a useful way of comparing the composition of the LRF rocks amongst themselves, and with other similar rock types, and have been used to characterize different geochemical groups. These plots also provide insight into petrogenetic processes as the elements behave in predictable ways during melting and fractional crystallization.

Based on trace element classification schemes, LRF volcanic rocks are subalkaline and compositions range in a Nb/Y vs. Zr/TiO_2 diagram (Fig. 6), from subalkaline basalt to rhyodacite, which is compatible with their major element compositions and mineralogy. In this diagram and in the Fe+Ti–Al–Mg cation plot, a compositional gap between tholeiitic andesite/basalt and dacite is observed (Fig. 7). The comparison of samples of the LRF with similar degrees of fractionation [i.e., Mg# = 100 × mol. MgO/(mol. MgO + mol. FeO_t)] reveals considerable variation in both the abundance of trace elements and the patterns on extended REE plots (Fig. 8). However, all of these tholeiitic rocks have pronounced negative Nb–Ta anomalies, indicating a subduction-related origin. As the HREE and HFSE (Ta, Nb, Zr, Hf and Ti) are not thought to be affected by the subduction-related component in arc magmas (Pearce and Parkinson, 1993), they can be used as guides to the composition of the mantle from which LRF rocks were derived. The positive slope of the HFSE increases with the degree of mantle depletion, and the abundance of the HREE (at equivalent degrees of fractionation) is a qualitative reflection of the degree of partial melting. These aspects are reflected in the normalized trace element ratios (Fig. 9): the $(Zr/Sm)_N$ reflects the extent and

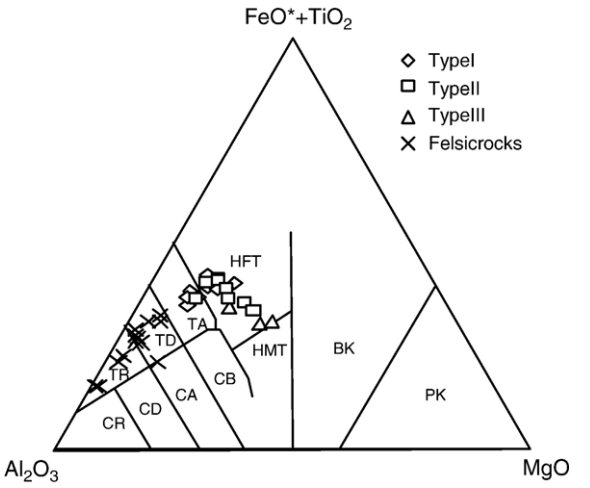

Fig. 7. Fe+Ti–Al–Mg cation plot (Jensen, 1976) of volcanic rocks of the Los Ranchos Fm. Abbreviations: PK = picritic komatiite; BK = basaltic komatiite; HMT = high-Mg tholeiite; HFT = high-Fe tholeiite; TA = tholeiitic andesite; TD = tholeiitic dacite; TR = tholeiitic rhyolite; CB = calc–alkaline basalt; CA = calc–alkaline andesite; CD = calc–alkaline dacite; and CR = calc–alkaline rhyolite.

nature of the Zr (and Hf) anomaly; and the $(La/Yb)_N$ reflects the degree of LREE enrichment or depletion. Lower values of both ratios indicate a more depleted mantle source prior to subduction-related metasomatism. The Mg# and TiO_2 content provide a qualitative reflection of the degree of fractionation and source depletion respectively, except where negative or positive Ti anomalies on extended REE plots indicate that the Ti content has been affected by crystal fractionation. Based on major and trace element variations, volcanic rocks of the LRF can be divided into three geochemical groups, although probably there are transitional compositions between them: type I, normal island arc tholeiites; type II, low-Ti and LREE-depleted island arc tholeiites; and type III, boninites. A type IV is assigned to felsic volcanic rocks separated of tonalite batholiths.

6.2.1. Type I, normal island arc tholeiites (IAT)

This group is represented by the massive flows, monogenetic autoclastic breccias and minor syn-volcanic intrusions of the upper basaltic unit (Table 1). These rocks have high-Fe tholeiitic basalt compositions (Fig. 7) and are quite fractionated (Mg# from 54 to 40). The

Fig. 8. Primitive mantle-normalized extended REE diagrams showing the variation of the trace element pattern at different Mg# in the mafic and felsic rocks of the Los Ranchos Fm. Different geochemical groups have been defined: (a) type I, normal island arc tholeiites (IAT); (b) type III, boninites; (c) type II, LREE-depleted intrusives; (d) examples of boninites (Murton et al., 1992; Pearce and Peate, 1995; Taylor and Nesbitt, 1995); (e) type II, LREE-depleted volcanics; (f) and (g) type IV, felsic volcanics; and (h) tonalite batholiths. Primitive mantle-normalizing values are from Sun and McDonough (1989).

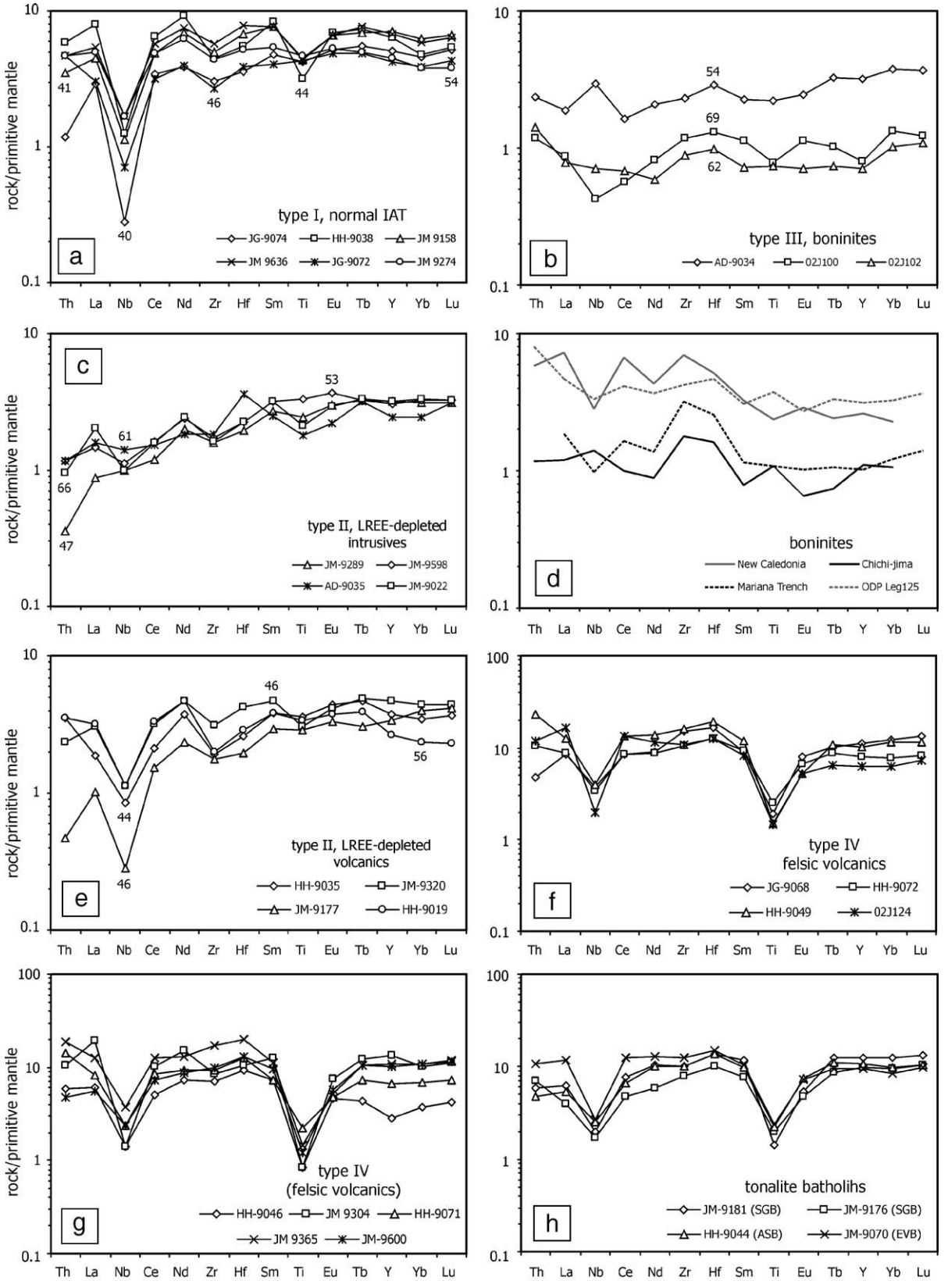
rock/primitive mantle
Th La Nb Ce Nd Zr Hf Sm Ti Eu Tb Y Yb Lu
a
type I, normal IAT
JG-9074 HH-9038 JM 9158
JM 9636 JG-9072 JM 9274
41
40
46
44
54
b
type III, boninites
AD-9034 02J100 02J102
54
69
62
c
type II, LREE-depleted intrusives
JM-9289 JM-9598
AD-9035 JM-9022
53
61
66
47
d
boninites
New Caledonia Chichi-jima
Mariana Trench ODP Leg125
e
type II, LREE-depleted volcanics
HH-9035 JM-9320
JM-9177 HH-9019
46
44
46
56
f
type IV felsic volcanics
JG-9068 HH-9072
HH-9049 02J124
g
type IV (felsic volcanics)
HH-9046 JM 9304 HH-9071
JM 9365 JM-9600
h
tonalite batholihs
JM-9181 (SGB) JM-9176 (SGB)
HH-9044 (ASB) JM-9070 (EVB)

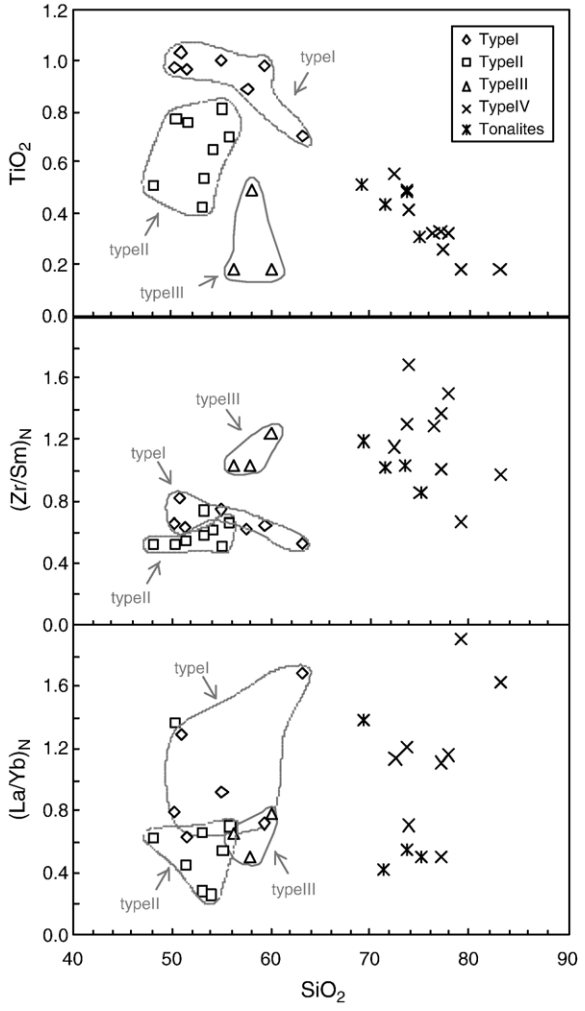

Fig. 9. SiO_2 vs. TiO_2, $(Zr/Sm)_N$ and $(La/Yb)_N$ variation diagrams for type I, normal island arc tholeiites (IAT); type II, LREE-depleted low-Ti IAT; type III, boninites; type IV felsic volcanic rocks and tonalites.

extended REE patterns (Fig. 8) are very similar to modern IAT (Saunders and Tarney, 1991; Pearce et al., 1992; Taylor and Nesbitt, 1995) and at similar absolute abundances (HREE 5–8 × primitive mantle). In particular, REE/HFSE ratios (e.g. La/Nb and Sm/Zr) are high in type I basalts relative to N-MORB compositions, which is typical of primitive island-arc tholeiites. They have slightly LREE-depleted to slightly LREE-enriched patterns ($[La/Yb]_N$ = 0.7–1.6; average 1.2; Fig. 9), pronounced negative Nb anomaly, slight negative Zr and positive Hf anomalies ($[Zr/Sm]_N$ = 0.3–0.8; average 0.62) and flat HREE. The TiO_2 content ranges between 0.8 and 1.0 wt.%. Average of initial $(^{87}Sr/^{86}Sr)_i$ ratio is 0.7044 calculated at t = 115 Ma. The $(\varepsilon_{Nd})_i$ values range from +9.2 to +10.06 (Table 2), suggesting a source dominated by depleted mantle.

6.2.2. Type II, low-Ti and LREE-depleted, island arc tholeiites (LREE-depleted IAT)

This group is represented by syn-volcanic mafic dykes, sills of microgabbro, irregular mafic bodies within the tonalite and diorite batholiths and the majority of mafic volcanic rocks in the lower basaltic unit of the LRF. These rocks have compositions ranging from high-Mg to high-Fe tholeiitic basalts, and extend to less fractionated compositions (Mg# from 66 to 44) than type I IAT. The extended REE patterns are similar to type I IAT, some with a pronounced negative Nb anomaly, but the absolute abundances are lower (HREE 2–5 × primitive mantle), the negative Zr and Hf anomalies are greater ($[Zr/Sm]_N$ = 0.5–0.8), and there is consistent LREE depletion ($[La/Yb]_N$ = 0.2–0.7; average 0.61). The TiO_2 content ranges between 0.4 and 0.8 wt.% and is considerably lower (average 0.64 wt.%) than that of type I IAT (average 0.93 wt.%). The $(^{87}Sr/^{86}Sr)_i$ values range between 0.70441 and 0.70568. Including mafic intrusive rocks, $(\varepsilon_{Nd})_i$ values range from +8.7 to +9.4, compatible with a source dominated by depleted mantle. The lower TiO_2 and HREE contents, and negative Zr and Hf anomalies suggest that the source for these rocks was more depleted than for type I, but they were probably produced by similar degrees of partial melting.

6.2.3. Type III, boninites

This group is represented by boninite flows and pillow lavas, with some volcanic breccias, present only in the lower basaltic unit of the LRF. Boninites have the composition of high-Mg tholeiitic basalt near basaltic komatiite, and include the least fractionated compositions of all the rocks sampled (Mg# 69 to 54). These rocks have slightly lower HREE abundances (0.7–3.2 × primitive mantle) than type II. However, they have flat to slightly LREE-enriched patterns ($[La/Yb]_N$ = 0.5–0.7) and strong positive Zr–Hf anomalies ($[Zr/Sm]_N$ = 1.0–1.3). This pattern is characteristic of modern-day boninites (Falloon and Crawford, 1991; Murton et al., 1992; Stern and Bloomer, 1992), and type III rocks are geochemically similar to group 3 low-Ca boninites (Crawford et al., 1989), including low CaO/Al_2O_3 (0.04–0.34) ratios relative to low-Ti IAT with similar degrees of fractionation. The low CaO/Al_2O_3 ratio and HREE abundances, and positive $(\varepsilon_{Nd})_i$ values (+3.4 to +5.6) are compatible with a source dominated by depleted mantle harzburgite. The $(^{87}Sr/^{86}Sr)_i$ values range from 0.70529 to 0.70534. Type III rocks are similar in composition to Cuban boninites described by Kerr et al. (1999).

6.2.4. Relationships between mafic igneous groups

Figs. 8 and 9 permit to compare the trace element characteristics between mafic volcanic rocks of the LRF, subvolcanic mafic dykes and gabbroic facies in the batholiths. Type II, low-Ti IAT volcanic rocks from the lower basaltic unit are similar in composition to massive gabbro from the Sabana Grande batholith (JM9177). Syn-magmatic doleritic dykes (AD9037; Table 1), microgabbros from El Valle batholith (JM9274) and hornblende diorite bodies intermingled with the tonalites in the batholiths, overlap with type I volcanic rocks from the upper basaltic unit. Therefore, the similarity in trace element compositions and ages argue for a genetic link between the mafic subvolcanic and volcanic rocks of the LRF and the gabbros in the tonalite batholiths.

6.3. Geochemical characteristics of felsic rocks

This group includes the felsic volcanic rocks of the intermediate rhyodacitic unit and the tonalite and subordinate quartz–diorite forming batholiths. In Fig. 7, felsic volcanic rocks and tonalites are classified as dacite to rhyolite, following the tholeiitic trend. The cumulative component of Ca-rich plagioclase and quartz observed in thin sections of tonalite gives place to a higher $CaO/(CaO+Na_2O)$ and Mg# (36–28) in these intrusives that in the felsic volcanic rocks (29–10). All felsic rocks are low in K ($K_2O<0.94$ wt.% in tonalites), TiO_2 (0.56–0.18 wt.%), P_2O_5 (<0.1 wt.%) and Zr, relative to typical calc-alkaline felsic rocks. Felsic volcanic rocks and tonalites have flat to slightly LREE-depleted REE patterns, which suggest a genetic link between them; i.e. felsic volcanic rocks are the extrusive equivalents of tonalite batholiths. Rhyodacites and rhyolites have $[La/Yb]_N=0.7–1.9$ (average 1.3) and tonalites and quartz–diorites $[La/Yb]_N=0.4–1.4$ (average 0.78). Therefore, they lack the moderate to strong LREE-enrichment typical of the calc-alkaline felsic rocks and thus are interpreted to have a tholeiitic affinity. The $(^{87}Sr/^{86}Sr)_i$ ratios extend from about 0.7029 to 0.7051 and $(\varepsilon_{Nd})_i$ values rang from +9.0 to +9.6 which are indicative of a source with long-term LREE depletion. High-SiO_2 (>70 wt.% SiO_2), low-K, felsic volcanism in intraoceanic arc systems are generally interpreted as the products of deep partial melting, as opposed to fractionation, of mafic rocks (Drummond and Defant, 1990; White et al., 1999; Tamura and Tatsumi, 2002). This is compatible with the gap of volcanic rocks with intermediate compositions in the LRF. The lack of Sr-rich and HREE-depleted dacitic compositions typical of adakites (Defant and Drummond, 1993) precludes a slab–melt origin for the felsic magmas. Processes of dehydration melting of underplated lower crust arc material, as has been proposed for the Kermadec arc (Smith et al., 2003), can generate by crustal anatexis the felsic magmatism in a developing intraoceanic arc.

6.4. Sr–Nd isotope systematics and interpretation

$^{87}Sr/^{86}Sr$ vs. $^{143}Nd/^{144}Nd$ variation in LRF displays a horizontal trend and is restricted to relatively high ε_{Nd} values (Fig. 10a; Table 2). Initial $(^{87}Sr/^{86}Sr)_i$ ratios are highly variable (0.7029–0.7057) at near constant $(\varepsilon_{Nd})_i$ (8.0–10.0), similar to altered rocks in modern intraoceanic arcs (Hergt and Hawkesworth, 1994) and consistent with seawater hydrothermal alteration (Kesler et al., 1990). In the LRF, $(^{87}Sr/^{86}Sr)_i$ values tend to decrease from type I IAT and boninites trough type II IAT to felsic rocks and gabbros. Acid leaching is generally believed to reduce the effects of seawater alteration by lowering of $^{87}Sr/^{86}Sr$ ratios, but the effects of some secondary phases like epidote or titanite are not affected, and values obtained from leached samples do not necessary reflect primary values. The $(^{144}Nd/^{143}Nd)_i$ ratios range between 0.51300 and 0.51295 and are relatively high, compatible with a source dominated by depleted mantle. Negative Nb anomalies on extended REE diagrams indicate a contribution to their chemistry from a subduction-related component. However, isotopic data are together indicative of minimal incorporation of sediment in LRF magmas, represented by the field of pelagic oceanic sediments of Hawkesworth et al. (1993).

The effect of mixing of subduction-related components with variably depleted mantle melt can be seen in the $^{147}Sm/^{144}Nd$ vs. $(\varepsilon_{Nd})_i$ diagram of the Fig. 10b. In this figure, the observed compositions and hypothetical end members sources calculated for the Lower Cretaceous following Swinden et al. (1990) are plotted. Hypothetical mantle sources are: DM (depleted mantle, not refractory), VDM (very depleted mantle, refractory), and the residue remaining after partial melting removes MORB from the DM source; SJM (subducted juvenile material); and SCM (subducted crustal material), based on composition of crustally derived sediments in modern oceans. The isotopic signatures of the type I IAT and microgabbro (JM9274) can be explained by mixing normal MORB-like depleted mantle (DM) with a component that has LREE-enrichment (i.e., low $^{147}Sm/^{144}Nd$), but positive ε_{Nd} values (i.e., long-term LREE-depletion). Such a signature could be generated by a subduction-related component that was in equilibrium with juvenile material (i.e., subducted oceanic

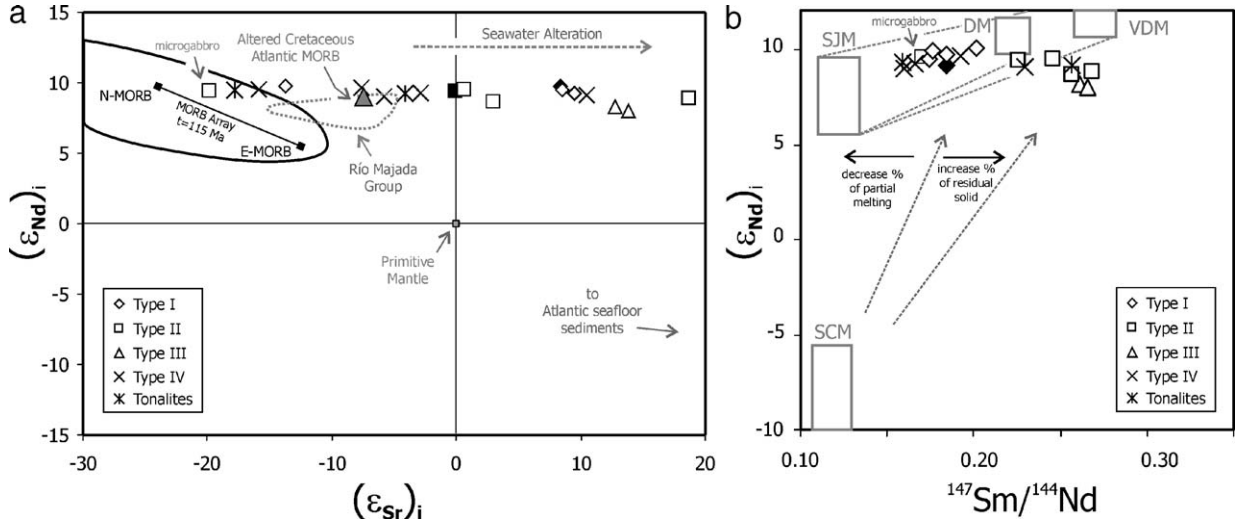

Fig. 10. (a) Initial Sr–Nd isotope ratios for unleached samples from the Los Ranchos Fm (open symbols) and compositionally equivalent rocks in the Amina Fm (black symbols; unpublished data). Initial ε_{Sr} and ε_{Nd} values calculated at $t=115$ Ma. MORB field and Altered Atlantic Cretaceous MORB are from Zindler and Hart (1986). Pelagic oceanic sediments are from Hawkesworth et al. (1993). Río Majada Group field ($t=110$ Ma) is volcanic phase 1 IAT lavas in central Puerto Rico (Upper Aptian to Lower Albian) from Jolly et al. (1998). (b) $^{147}Sm/^{144}Nd$ vs. $(\varepsilon_{Nd})_i$ diagram for the same rocks showing the various mantle and subduction components interpreted to be involved in its petrogenesis. Hypothetical mantle sources are: DM=depleted mantle; VDM=very depleted mantle; SJM=subducted juvenile material; and SCM=subducted crustal material. Discontinuous lines schematically illustrate mixing trends. See text for explanation.

crust with little or no pelagic sediment). The low-Ti, LREE-depleted IAT compositions can also be explained by mixing very depleted mantle (modeled VDM or more depleted) and LREE-enriched fluids from subducted juvenile material. The boninites plot within the array defined by the low-Ti IAT, which shows that their LREE-enriched signature is not derived from a source region with long-term LREE-enrichment, but developed during their generation. The felsic rocks have ($^{147}Sm/^{144}Nd)_i$ values between 0.16 and 0.26, with a very narrow range of $(\varepsilon_{Nd})_i$ values (+9.2 to +9.6). The variation in ε_{Nd} reflects that of the mafic rocks from which they were derived, with minor incorporation of subducted continental material. The range in $^{147}Sm/^{144}Nd$ reflects the broad degree of fractionation of these two elements during the partial melting.

7. Discussion and conclusions

7.1. Mantle and slab contributions

Because of their primitive character, the least fractionated samples of the LRF allow to evaluate primary melt compositions. Previous work (Donnelly et al., 1990; Kesler et al., 1990; Lewis et al., 2000, 2002) and the data presented in this study have established that these relatively low fractionated mafic rocks were generated in the mantle wedge above a subduction zone, below the Early Cretaceous Caribbean Island arc. In this setting, the concentration of a given element in magmas formed in a subduction zone is determined by the partial melting and crystal fractionation history of a source containing both mantle-derived and subducting slab-derived components. The HFSE (Nb, Ta, Hf, Zr, Y, Ti) are considered to remain immobile during slab-fluxing processes and their values should reflect compositions in the mantle wedge, whereas LILE (Rb, Ba, Sr, Cs, Th, U, Pb, Na, K) and LREE and MREE (La, Ce, Nd, Sm, Eu) enrichments are consistent with slab involvement (McCulloch and Gamble, 1991; Pearce and Parkinson, 1993; Pearce and Peate, 1995). A mantle origin is also ascribed to the HREE (Tb, Yb, Lu) and the compatible elements (Cr, Ni, Co, Mg, Fe, Mn, Sc, V, Al, Ca), which are not affected by the subduction component (i.e., they are also conservative with respect to the mantle source). Therefore, the relative contribution of the mantle and slab can be evaluated using N-MORB-normalized patterns of a suite of trace elements dominantly extracted from one or the other of these sources (Pearce, 1983). A diagram for the least representative fractionated samples of the LRF (Fig. 11) demonstrates that primary mantle compositions of the LILE and LREE are estimated by extrapolation of a "baseline" connecting the mantle-derived element, following a method similar to that proposed by Pearce and Parkinson (1993). In these diagrams, the area above

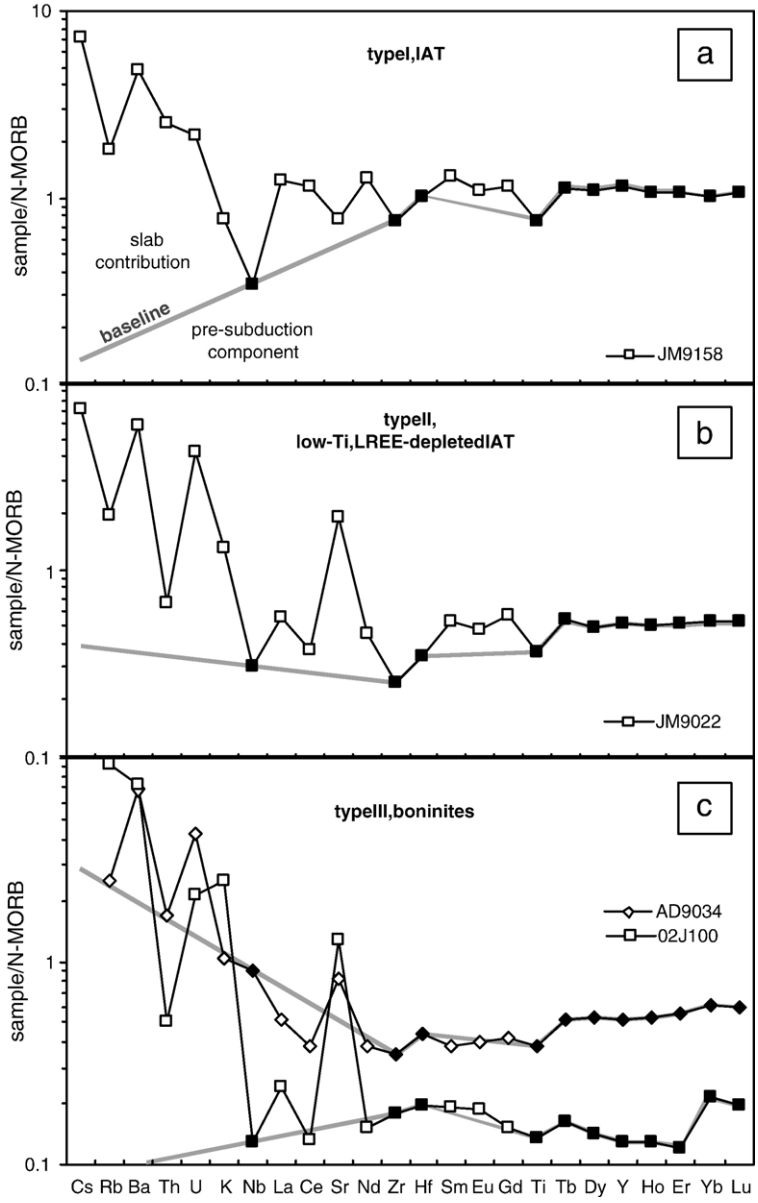

Fig. 11. MORB-normalized trace element plot for low fractionated rocks of the different geochemical groups defined in the Los Ranchos Fm. Elements thought to be derived primarily from the mantle wedge are shown as black squares, whereas those which involve a significant subduction component are shown as white squares. The left side of the baseline indicates the extrapolated abundances in the mantle wedge of those elements mainly derived from the subducting slab. Normalizing values and order of relative incompatibility with a fertile spinel–lherzolite mantle are taken from Sun and McDonough (1989) and Pearce and Parkinson (1993). See text for discussion.

the baseline represents the slab contribution of a given element. In an idealized case where concentrations of the HFSE and HREE are determined only by the degree of partial melting, the baseline would form a trend parallel to the N-MORB normalizing value (parallel to the *x*-axis). An increase of the degree of partial melting reduces HFSE abundances, forcing the baseline down to the *x*-axis.

As shown in Fig. 11, melting variations can gave decrease the baseline between IAT, LREE-depleted IAT and boninites, but are insufficient to explain the relative depletions or enrichments of various elements. For all mafic types, the slab contribution above the baseline includes variable proportions of LILE, LREE and MREE elements. Experimental studies of partition coefficients between hydrous fluids and mantle mineral

assemblages (e.g., Brenan et al., 1995), and the relationship between bulk partition coefficients and ionic radius (summarized by Pearce and Peate, 1995), suggest that these elements can only be mobilized by aqueous fluids and that the degree of enrichment in such fluids should increase from MREE through LREE to LILE. Therefore, the mafic volcanic rocks of the LRF are interpreted to have been produced by variable degrees of melting by fluxing of a depleted mantle with subduction-related hydrous fluids. The degree of melting increases from IAT to LREE-depleted IAT and boninites, as indicated in the decrease in HFSE and HREE. The progressive lower concentration in Ti and HREE, with the negative anomalies in Zr–Hf, also establishes that the mantle source for these rocks was more depleted. Ti can be affected by moderated fractionation in the sample JM9158 of type I IAT (Mg# ~40) or, alternatively, to require the existence of residual amphibole in the mantle wedge.

In boninites, low HREE abundances (02J100 and 02J102) indicate a source dominated by strongly depleted mantle harzburgite. The enrichment in Zr and Hf relative to Nb seen in LRF boninites, also described in other boninites (e.g. Chichi-jima and Mariana Trench; Fig. 8), can be the result of melting of the slab in amphibolite facies. This interpretation is compatible with the greater degree of enrichment of the LREE and the non-conservative behaviour of Nb. A comparison of the distribution coefficients for these elements between mantle/melt and mantle/aqueous fluid (e.g., Brenan et al., 1995) shows that melts are much more effective at extracting the LREE and at extracting HFSE (Ti, Zr, Hf, Nb and Ta) from the mantle. Residual amphibole present during melting would reverse the usual order of incompatibility of Zr (and Hf) and Nb (and Ta) resulting in the positive Zr and Hf anomalies characteristic of these boninites. In the boninite AD9034, however, the upward slope of the left side of the diagram represents enrichment of Nb (and Hf) in the mantle wedge that cannot be attributed to the aqueous fluids since they do not have the appropriate composition. This enrichment may be related to an ocean–island–basalt-like (plume) component (e.g. Stern et al., 1991), since in a context of intra-oceanic subduction the influence of subcontinental lithosphere in Nb enrichment is discarded (Pearce, 1983).

The input of various elements in the mafic lavas from the subducting slab can be investigated using trace element ratio plots normalized to the highly incompatible element Yb (Pearce and Peate, 1995; Peate et al., 1997), as included in Fig. 12. On a Zr/Yb vs. Nb/Yb diagram, LRF samples plot along the N-MORB array and bellow, from the average N-MORB composition to progressively more depleted sources, support a mantle origin for almost all Zr. The low Zr/Yb and Nb/Yb ratios indicate variable depletion of the mantle source compared with N-MORB, from IAT, to LREE-depleted IAT and boninites in relation to the melting history. The subduction contribution for other elements such as Th, La and Nd can be quantified according to the method described by Pearce and Peate (1995), provided that no Nb or Yb has a subduction origin. In Fig. 12, the subduction vector extends vertically from the MORB array, with the actual subduction contribution estimated by contour lines drawn parallel to the MORB trend. The diagram reveal that the subduction contributions for Th, La and Nd range up to 90%, 80% and 75% for type I, respectively, being generally smaller for type II and boninites. As type I mafic volcanics are characteristic of the upper basaltic unit in the LRF and type II and boninitic volcanics of the lower basaltic unit, this variation suggests a more efficient mechanism of fluid (and melts) fluxing from the subducting slab with time. However, the scatter in the data parallel to the subduction vector may also be attributed to heterogeneous slab flux, and the scatter parallel to the MORB trend may be related to variations in melting history, fractional crystallization, and, given the low abundances of HFSE in most samples, analytical error.

7.2. Partial melting and fractional crystallization

Pearce and Parkinson (1993) show that simple petrogenetic modeling of processes operating in the source region can be carried out by using a highly compatible element such as Cr and an immobile incompatible element such as Yb. Yb and Cr may be used as indices of partial melting and fractionation, respectively, as their abundances in the source regions for most magmas probably approximated primordial mantle. A Cr vs. Yb diagram show the extrapolation of fractionation trends back to an empirically derived plagioclase crystallization line and thence to the melting curve along the mafic phase crystallization line (Fig. 13a). For types I and II IAT of the LRF, this diagram support a high degree (15–25%) of partial melting of a FMM (fertile MORB mantle) source or low degree (10–1%) melting of a 10% depleted FMM, but unrealistic high degree of partial melting of FFM for boninites (>40% in spinel-out conditions). Thus, this diagram provides further evidence that source depletion (25–15% of FMM) must play a major role in the genesis of boninites. It is also evident from Fig. 13a that LREE-depleted IAT and boninites can be produced by

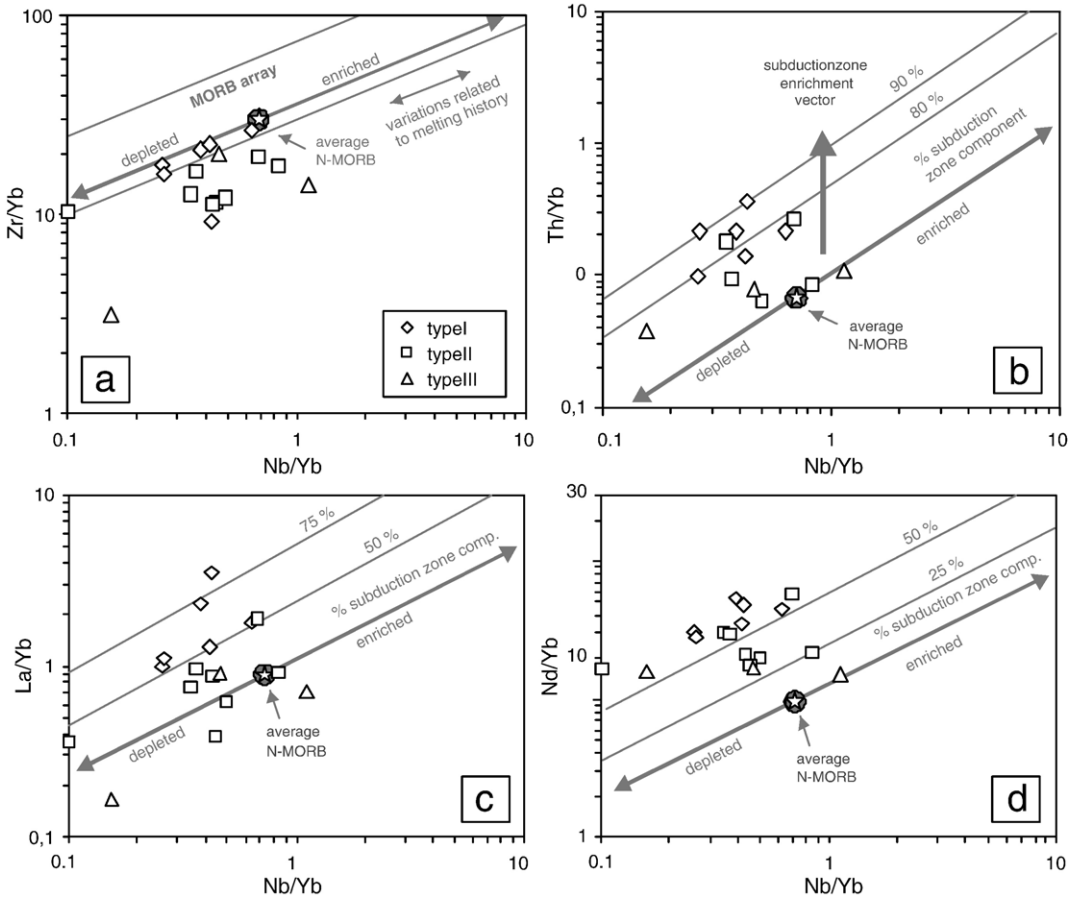

Fig. 12. Trace element ratio plots of (a) Zr/Yb, (b) Th/Yb, (c) La/Yb and (d) Nd/Yb vs. Nb/Yb for mafic volcanic rocks of the Los Ranchos Fm. The sloped solid line shows patterns of enrichment and depletion of an average N-MORB mantle, and the broken lines represent contours of % subduction zone contribution for a given element in the mantle (Pearce and Peate, 1995). Vectors for variations caused by subduction zone enrichment and melting history are also illustrated.

fractionation of only mafic phases, which is consistent with the presence of olivine and pyroxene phenocrysts in the lavas of the lower basaltic unit; whereas IAT require, in addition, the crystallization of plagioclase at low Cr concentrations, which agree with the abundant occurrence of plagioclase phenocrysts in the upper basaltic unit.

In Fig. 13b, a trace element plot of Nb and Yb normalized to 9.0 wt.% MgO ($Nb_{9.0}$ vs. $Yb_{9.0}$) allows the effects of partial melting to be separated from those of source depletion or enrichment (Pearce and Parkinson, 1993; Peate et al., 1997). To build this plot for LRF volcanics, samples of types I and II with MgO >5 wt.% have been removed and the fields of IAT and N-MORB compositions compiled by Pearce and Parkinson (1993) have been included. Although magmas at 9 wt.% MgO are not primary, they lie on the olivine–Cr spinel cotectic and are close to primary compositions for incompatible trace elements, which allow minimisation of the effects of fractional crystallization. Fig. 13b supports the existence of fertile MORB mantle (FMM) or more depleted mantle sources for IAT of the LRF. This diagram corroborates the moderate to very high melting proportions (5–30% of FMM) required by type II and moderate melting proportions (about 5–10%) for type I, although the separation of each mafic type into discrete melt populations is not in evidence by the scarce of low fractionated rocks. Boninites are not included in Fig. 13b since they can have a slab-related Nb enrichment. As is observed in Fig. 13b, the percentage of partial melting in some LREE-depleted IAT of the lower basaltic unit can be very high, ranging between 15% and 35%. There are no IAT compositions that fall bellow the melting trend for 5% source depletion, including LRF mafic volcanics, which is consistent with the maximum of about of 3% of melt removed from the

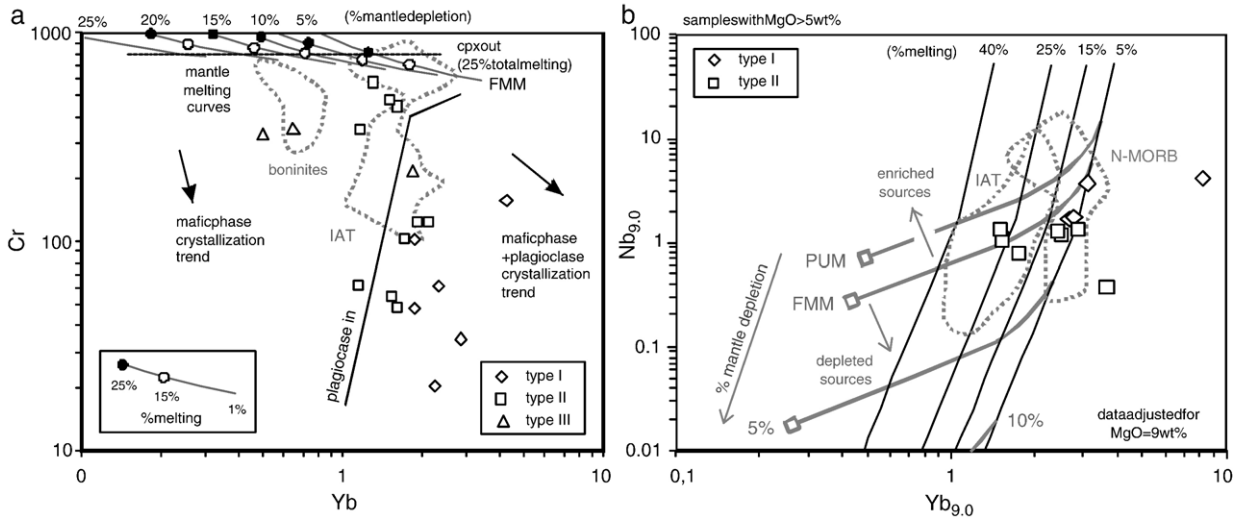

Fig. 13. (a) Cr vs. Yb diagram, assuming melting in spinel lherzolite facies (Pearce and Parkinson, 1993), showing compositional variation in mafic volcanic rocks of the Los Ranchos Fm. and the pathways that connect them to primordial mantle composition. As shown by the position of the "plagioclase-in" line, plagioclase is a crystallizing phase only in type I and fractionated type II lavas. The variation within each geochemical group is subparallel to the *y*-axis (Cr) and is explained by differences in degree of fractionation, whereas variation between groups is subparallel to the *x*-axis (Yb), consistent with differences in degree of partial melting. (b) Nb vs. Yb plot, with trace element compositions normalized to MgO=9 wt.% following the method described by Pearce and Parkinson (1993). Contours for partial melting and enrichment or depletion are after Pearce and Parkinson (1993). FMM=fertile MORB mantle; PUM=primitive upper mantle composition. See text for further discussion.

mantle during the depletion processes even in the most extremely depleted islands of the Tonga, Kermadec and South Sandwich arcs, with thin lithosphere and associated active backarc basins.

7.3. Tectonic setting and evolution of volcanism

Recently, Kesler et al. (2005) describes the meaning of the primitive island arc volcanic sequences in terms of contrasting models for Albian plate tectonic configuration of the Caribbean region. In this tectonic context, the magmatic rocks of the lower basaltic unit of the LRF are predominantly low-Ti, high-Mg, LREE-depleted IAT and boninites extruded in a submarine environment. The abundance of syn-volcanic dykes and sills of microgabbros intruded the lower basaltic unit suggested that the lower levels of the unexposed basement was probably extended, by analogous structures imagined by seismic reflection profiles in the mid-forearc of the south Sandwith arc (Larter et al., 2003). Taken together, the timing, structural setting and geochemical characteristics of volcanic rocks and dykes suggest an extensional, supra-subduction zone setting during the earliest stages of Early Cretaceous Caribbean Island arc development. Higher in the stratigraphic sequence of the LRF, there is a clear temporal evolution to IAT of the upper basaltic unit that grade to an upper sequence of lithic tuffs, volcanic sandstone and fossiliferous sediments. Therefore, LRF rocks fit the petrogenetic models proposed for subduction zone infancy, as Izu–Bonin–Mariana system forearc (Pearce et al., 1992; Stern and Bloomer, 1992; Bloomer et al., 1995), where generation of boninite magmas is ascribed to high-temperature melting of shallow, depleted mantle associated with the initiation of subduction of young, buoyant ocean crust. Subsequently, tholeiitic and more calc–alkalic magmas are generated when older, denser oceanic crust is subducted at a greater angle in an established subduction zone, resulting in melting of deeper, less depleted mantle. Although forearc setting is characterized by boninitic rocks in the Izu–Bonin–Mariana arc, stratigraphic data and geochemical/isotopic characteristics of the earliest

Fig. 14. Schematic tectonomagmatic model for the evolution of the volcanic rocks of the Los Ranchos Fm and intrusion of tonalite batholiths, based on the model of Stern and Bloomer (1992). (1) initiation of subsidence and high degrees of partial melting of fertile MORB mantle to produce trace element poor normal IAT magmas and very depleted mantle (VDM) residue; (2) continued subsidence and production of LREE-depleted IAT and boninites by hydrous melting of residual VDM mantle, and with the beginning of subduction melting at the base of the crust to produce tonalitic magmas; (3) stabilization of the magmatic front by continued subduction, lateral migration of fertile MORB mantle to the melting zone to produce less depleted and normal IAT and the migration of the locus of extension to a backarc position.

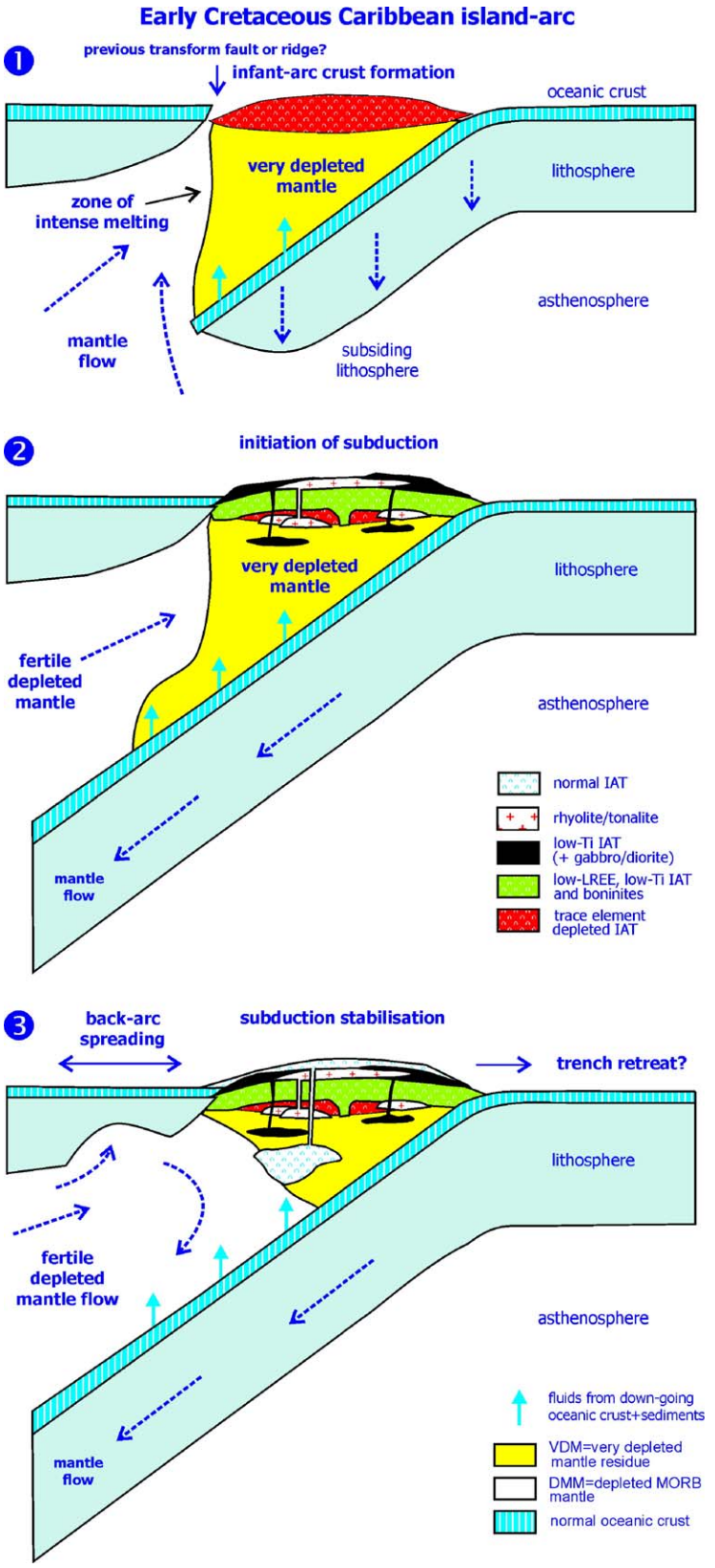
Early Cretaceous Caribbean island-arc
1
previous transform fault or ridge?
infant-arc crust formation
oceanic crust
very depleted mantle
lithosphere
zone of intense melting
asthenosphere
mantle flow
subsiding lithosphere
2
initiation of subduction
very depleted mantle
lithosphere
fertile depleted mantle
asthenosphere
mantle flow
normal IAT
rhyolite/tonalite
low-Ti IAT (+ gabbro/diorite)
low-LREE, low-Ti IAT and boninites
trace element depleted IAT
3
back-arc spreading
subduction stabilisation
trench retreat?
lithosphere
fertile depleted mantle flow
asthenosphere
mantle flow
fluids from down-going oceanic crust+sediments
VDM=very depleted mantle residue
DMM=depleted MORB mantle
normal oceanic crust

mafic rocks of the LRF and intrusives, established that the LREE-depleted IAT and boninites are temporally, spatially and probably genetically related. Following the model of Stern and Bloomer (1992), initiation of subsidence and high degrees of partial melting of MORB mantle produce trace element-poor normal IAT magmas and very depleted mantle residue (VDM). Continued subsidence produce type II LREE-depleted IAT and type III boninites of lower basaltic unit by hydrous melting of VDM (Fig. 14a). In favor of this interpretation are the moderate to very high melting proportions (5–30% of FMM; Fig. 13) required by type II mafic rocks and the very depleted nature of boninites. In the LRF, the evolution of volcanics with time was accompanied by a change in geochemical character, toward less depleted compositions recorded in the upper basaltic unit. This is interpreted to result from addition of DMM to the region by its moving laterally into the area of extension (Fig. 14b), once the subducting slab prohibits significant upwelling. In this case, without the added effect of decompression, the new fertile mantle wedge would undergo degrees of partial melting typical of N-MORB (5–15% in Fig. 13b), thus generating type I normal IAT. The rapid rate of crust formation proposed for subduction zone infancy (Stern and Bloomer, 1992) provides an explanation for the formation of rhyolites (and tonalite batholiths) within several million years of the depleted mafic sequence, by melting of the depleted rocks at the base of the thickened arc crust (Fig. 14c; see also White et al., 1999). Volcanic rocks of the upper basaltic unit and late mafic to intermediate dykes which crosscut all other units have the geochemical characteristics of IAT, and are interpreted to represent a normal island arc volcanism, after stabilization of the volcanic front and migration the locus of extension to a backarc position.

Acknowledgements

The authors would like to thank John Lewis (George Washington University) and Gren Draper (Florida International University) for his introduction to the area, initial field-work and continued discussions and advice on the petrology and geochemistry of arc-related volcanic rocks in the Dominican Republic, and the LRF in particular. Dominique Weis (University of British Columbia) is also thanked for the isotopic analysis and a previous revision of the paper. Thanks also go to S. Foley and two anonymous reviewers for the careful review of the manuscript. This work form part of the geothematic cartographic project of the Dominican Republic funded by the SYSMIN program of the European Union and also received financial aid from MCYT projects BTE-2002-00326 and CGL2005-02162/BTE.

Appendix A. Supplementary data

Supplementary data associated with this article can be found, in the online version, at doi:10.1016/j.lithos.2006.02.001.

References

Bédard, J.H., 1999. Petrogenesis of Boninites from the Betts Cove Ophiolite, Newfoundland, Canada: identification of subducted source components. Journal of Petrology 40, 1853–1889.

Bédard, J.H., Lauziere, K., Tremblay, A., Sangster, A., 1998. Evidence for forearc seafloor-spreading from the Betts Cove Ophiolite, Newfoundland: oceanic crust of boninitic affinity. Tectonophysics 284, 233–245.

Bienvenu, P., Bougault, H., Joron, J.L., Treuil, M., Demitriev, L., 1990. REE/non REE element hygromagmaphile element fractionation. Chemical Geology 82, 1–14.

Bloomer, S.H., Hawkins, J.W., 1987. Petrology and geochemistry of boninite series volcanic rocks from the Marianna Trench. Contributions to Mineralogy and Petrology 89, 256–262.

Bloomer, S.H., Taylor, B., MacLead, C.J., Stern, R.J., Freyer, P., Hawkins, J.W., Johnson, L., 1995. Early arc volcanism and the ophiolitic problem: a perspective from drilling in the western Pacific. In: Taylor, B., Natlend, J. (Eds.), Active Margins and Marginal Basins of the Western Pacific. Geophysical Monograph, vol. 88, pp. 1–24.

Bourdon, L., 1985. La Cordillère Orientale Dominicaine (Hispaniola, Grandes Antilles): un arc insulaire Crétacé polystructure. Thèse Doctorale. Université Pierre et Marie Curie, Paris.

Bowin, C., 1975. The geology of Española. In: Naim, A., Stehli, F. (Eds.), The Ocean Basins and Margins: The Gulf of Mexico and the Caribbean, vol. 3. Plenum Press, New York, pp. 501–552.

Brenan, J.M., Shaw, H.F., Ryerson, F.J., Phinney, D., 1995. Mineral–aqueous fluid partitioning of trace elements at 900 °C and 2.0 GPa: constraints on the trace element chemistry of mantle and deep crustal fluids. Geochimica et Cosmochimica Acta 59, 3331–3350.

Brown, A.V., Jenner, G.A., 1989. Geologic setting, petrology and chemistry of Cambrian boninite and low-Ti lavas in western Tasmania. In: Crawford, A.J. (Ed.), Boninites and Related Rocks. Unwin Hyman, London, pp. 233–263.

Clift, P.D., Dixon, J.E., 1998. Jurassic ridge collapse, subduction initiation and ophiolite obduction in the southern Greek Tethys. Eclogae Geologicae Helveticae 91, 123–138.

Crawford, A.J., Falloon, T.J., Green, D.H., 1989. Classification, petrogenesis and tectonic setting of boninites. In: Crawford, A.J. (Ed.), Boninites and Related Rocks. Unwin Hyman, London, pp. 1–49.

Cumming, G.L., Kesler, S.E., 1987. Lead isotopic composition of the oldest volcanic rocks of the eastern Greater Antilles island arc. Chemical Geology 65, 15–23.

Defant, M.J., Drummond, M.S., 1993. Mount St. Helens: potential example of the partial melting of the subducted lithosphere in a volcanic arc. Geology 21, 547–550.

Dolan, J., Mullins, H., Wald, D., 1998. Active tectonics of the north-central Caribbean region: oblique collision, strain partitioning and

opposing slabs. In: Dolan, J., Mann, P. (Eds.), Active Strike–Slip and Collisional Tectonics of the Northern Caribbean Plate Boundary Zone in Hispaniola. Geological Society American Special Paper, vol. 326, pp. 1–61.

Donnelly, T.W., Beets, D., Carr, M.J., Jackson, T., Klaver, G., Lewis, J., Maury, R., Schellenkens, H., Smith, A.L., Wadge, G., Westercamp, D., 1990. History and tectonic setting of Caribbean magmatism. In: Dengo, G., Case, J.E. (Eds.), The Caribbean Region. The Geology of North America. Geological Society of America, Boulder, CO, pp. H, 339–H, 374.

Draper, G., Mann, P., Lewis, J.F., 1994. Hispaniola. In: Donovan, S.K., Jackson, T.A. (Eds.), Caribbean Geology: An Introduction. University of the West Indies Publishers Association, Jamaica, pp. 129–150.

Drummond, M.S., Defant, M.J., 1990. A model for trondhjemite–tonalite–dacite genesis and crustal growth via slab melting: archean to modern comparisons. Journal of Geophysical Research 95, 21503–21521.

Falloon, T.J., Crawford, A.J., 1991. The petrogenesis of high calcium boninite lavas from the northern Tonga ridge. Earth and Planetary Science Letters 102, 375–394.

Gradstein, F.M., Ogg, J.G., Smith, A.G., 2004. A Geologic Time Scale 2004. Cambridge University Press. 610 pp.

Hawkesworth, C.J., Gallager, K., Hergt, J.M., McDermott, F., 1993. Mantle and slab contributions in arc magmas. Annual Review of Earth and Planetary Sciences 21, 175–204.

Hergt, J.M., Hawkesworth, C.J., 1994. Pb-, Sr- and Nd-isotopic evolution of the Lau Basin: implications for mantle dynamics during backarc opening. In: Hawkins, J., Parsons, L., Allan, J. (Eds.), Proceedings of the Ocean Drilling Program, Scientific Results, vol. 135, pp. 505–517.

Humphris, S.E., Thompson, G., 1978. Hydrothermal alteration of oceanic basalts by seawater. Geochimica et Cosmochimica Acta 42, 107–125.

Jensen, L.S., 1976. A new cation plot for classifying subalkalic volcanic rocks. Miscellaneous Paper 66, Ontario Department of Mines, Canada.

Jolly, W.T., Lidiak, E.G., Dickin, A.K., Wu, T.W., 1998. Geochemical diversity of Mesozoic island arc tectonic blocks in eastern Puerto Rico. In: Lidiak, E.G., Larue, D.K. (Eds.), Tectonics and Geochemistry of the Northeastern Caribbean. Geological Society of America Special Paper, vol. 322, pp. 67–98.

Kerr, A.C., Iturralde-Vinent, M.A., Saunders, A.D., Babbs, T.L., Tarney, J., 1999. A new plate tectonic model of the Caribbean: implications from a geochemical reconnaissance of Cuban Mesozoic volcanic rocks. Geological Society of America Bulletin 111, 1581–1599.

Kesler, S.E., Lewis, J.F., Jones, L.M., Walker, R.L., 1977. Early island-arc intrusive activity, Cordillera Central, Dominican Republic. Contributions to Mineralogy and Petrology 65, 91–99.

Kesler, S.E., Russell, N., Polanco, J., McCurdy, K., Cumming, G.J., 1990. Geology and geochemistry of the Early Cretaceous Los Ranchos Formation, central Dominican Republic. In: Mann, P., Draper, G., Lewis, J.F. (Eds.), Geologic and Tectonic Development of the North America–Caribbean Plate Boundary in Española. Geological Society of America Special Paper, vol. 262, pp. 187–201.

Kesler, S.E., Russell, N., McCurdy, K., 2003. Trace-element content of the Pueblo Viejo precious-metal deposits and their relation to other high-sulfidation epithermal systems. Mineralium Deposita 38, 668–682.

Kesler, S.E., Campbell, I.H., Allen, Ch.M., 2005. Age of the Los Ranchos Formation, Dominican Republic: timing and tectonic setting of primitive island arc volcanism in the Caribbean region. Geological Society of America Bulletin 117, 987–995.

Larter, R.D., Vanneste, L.E., Morris, P., Smyth, D.K., 2003. Tectonic evolution and structure of the South Sandwich arc. In: Larter, R., Leat, P.T. (Eds.), Intra-Oceanic Subduction Systems: Tectonic and Magmatic Processes. Geological Society London Special Publication, vol. 219, pp. 255–284.

Lebrón, M.C., Perfit, M.R., 1994. Petrochemistry and tectonic significance of Cretaceous island-arc-rocks, Cordillera Oriental, Dominican Republic. Tectonophysics 229, 69–100.

Lewis, J.F., Draper, G., 1990. Geological and tectonic evolution of the northern Caribbean margin. In: Dengo, G., Case, J.E. (Eds.), The Geology of North America, The Caribbean Region. Geological Society of America, Colorado, pp. 77–140.

Lewis, J.F., Astacio, V.A., Espaillat, J., Jiménez, J., 2000. The occurrence of volcanogenic massive sulfide deposits in the Maimon Formation, Dominican Republic: the Cerro de Maimón, Loma Pesada and Loma Barbuito deposits. In: Sherlock, R., Barsch, R., Logan, A. (Eds.), VMS Deposits of Latin America. Geological Society of Canada Special Publication. 223–249 pp.

Lewis, J.F., Escuder Viruete, J., Hernaiz Huerta, P.P., Gutiérrez, G., Draper, G., Pérez Estaún, A., 2002. Subdivisión geoquímica del Arco Isla Circum-Caribeño, Cordillera Central Dominicana: implicaciones para la formación, acreción y crecimiento cortical en un ambiente intraoceánico. Acta Geologica Hispanica 37, 81–122.

MacLachlan, K., Dunning, G.R., 1998. U–Pb ages and tectonomagmatic relationships of Early Ordovician low-Ti tholeiites, boninites and related plutonic rocks in Central Newfoundland, Canada. Contributions to Mineralogy and Petrology 133, 235–258.

Mann, P., 1999. Caribbean sedimentary basins: classification and tectonic setting from Jurassic to present. In: Mann, P. (Ed.), Caribbean Basins. Sedimentary Basins of the Word, vol. 4, pp. 3–31.

Mann, P., Draper, G., Lewis, J.F., 1991. An overview of the geologic and tectonic development of Española. In: Mann, P., Draper, G., Lewis, J.F. (Eds.), Geologic and Tectonic Development of the North America–Caribbean Plate Boundary in Española. Geological Society of America Special Paper, vol. 262, pp. 1–28.

McCulloch, M.T., Gamble, J.A., 1991. Geochemical and geodynamical constraints on subduction zone magmatism. Earth and Planetary Science Letters 102, 358–374.

Meijer, A., 1980. Primitive arc volcanism and boninitic series: examples from Western Pacific island arcs. In: Hayes, D.E. (Ed.), The Tectonic and Geologic Evolution of SE Asian Seas and Islands. American Geophysical Union Geophysical Monograph, vol. 23, pp. 269–282.

Murton, B.J., Peate, D.W., Arculus, R.J., Pearce, J.A., Van der Laan, 1992. Trace-element geochemistry of volcanic rocks from Site 786: the Izu–Bonin forearc. In: Fryer, P., Pearce, J.A., Stokking, L.B. (Eds.), Proceedings of the Ocean Drilling Program, Scientific Results, vol. 125, pp. 211–235.

Nelson, C.E., 2000. Volcanic domes and gold mineralization in the Pueblo Viejo district, Dominican Republic. Mineralium Deposita 35, 511–525.

Pearce, J.A., 1983. The role of sub-continental lithosphere in magma genesis at destructive plate margins. In: Hawkesworth, C.J., Norry, M.J. (Eds.), Continental Basalts and Mantle Xenoliths. Shiva, Nantwich, pp. 230–249.

Pearce, J.A., Parkinson, I.J., 1993. Trace element models for mantle melting: application to volcanic arc petrogenesis. In: Pritchard, H.M., Alabaster, T., Harris, N.B.W., Nearly, C.R. (Eds.),

Magmatic Processes and Plate Tectonics. Geological Society of London Special Publication, vol. 76, pp. 373–403.

Pearce, J.A., Peate, D.W., 1995. Tectonic implications of the composition of volcanic arc magmas. Earth and Planetary Science Annual Review 23, 251–285.

Pearce, J.A., van der Laan, S.R., Arculus, R.J., Murton, B.J., Ishii, T., Peate, D.W., Parkinson, I.J., 1992. Boninite and harzburgite from Leg 125 (Bonin–Mariana Fore-arc): a case study of magma genesis during the initial stages of subduction. In: Fryer, P., Pearce, J.A., Stocking, L.B. (Eds.), Proceedings Ocean Drilling Program, Scientific Results, vol. 125, pp. 623–659.

Peate, D.W., Pearce, J.A., Hawkesworth, C.J., Colley, H., Edwards, C. M.H., Hirose, K., 1997. Geochemical variations in Vanuatu arc lavas: the role of subducted material and a variable mantle wedge composition. Journal of Petrology 38, 1331–1358.

Smith, I.E.M., Worthington, T.J., Steward, R.B., Price, R.C., Gamble, J.A., 2003. Felsic volcanism in the Kermadec arc, SW Pacific: crustal recycling in an oceanic setting. In: Laster, R.B., Leat, P.T. (Eds.), Intraoceanic Subduction Systems: Tectonic and Magmatic Processes. Geological Society London Special Publication, vol. 219, pp. 99–118.

Spadea, P., Scarrow, J.H., 2000. Early Devonian boninites from the Magnitogorsk arc, southern Urals (Russia): implications for early development of a collisional orogen. In: Dilek, Y., Moores, E.M., Elthon, D., Nicolas, A. (Eds.), Ophiolites and Oceanic Crust: New Insights from Field Studies and the Ocean Drilling Program. Geological Society of America Special Paper, vol. 349, pp. 461–472.

Stern, R.J., Bloomer, S.H., 1992. Subduction zone infancy: examples from the Eocene Izu–Bonin–Mariana and Jurassic California arcs. Geological Society of America Bulletin 104, 1621–1636.

Stern, R.J., Morris, J., Bloomer, S.H., Hawkins, J.W., 1991. The source of the subduction component in convergent margin magmas: race element and radiogenic isotope evidence from Eocene boninites, Mariana forearc. Geochimica et Cosmochimica Acta 55, 1467–1481.

Sun, S.S., McDonough, W.F., 1989. Chemical and isotopic systematics of oceanic basalts: implications for mantle compositions and processes. In: Saunders, A.D., Norry, M.J. (Eds.), Magmatism in the Ocean Basins. Geological Society Special Publication, vol. 42, pp. 313–345.

Swinden, H.S, Jenner, G.A., Fryer, B.J., Hertogen, J., Roddick, J. C., 1990. Petrogenesis and paleotectonic history of the Wild Bight Group, an Ordovician rifted island arc in central Newfoundland. Contributions to Mineralogy and Petrology 105, 219–241.

Tamura, Y., Tatsumi, Y., 2002. Remelting of an andesitic crust as a possible origin for rhyolitic magma in oceanic arcs: an example from the Izu–Bonin arc. Journal of Petrology 43, 1029–1047.

Taylor, R.N., Nesbitt, R.W., 1995. Arc volcanism in an extensional region on initiation of subduction: a geochemical study of Hawajima, Bonin Islands, Japan. In: Smelie, J.L. (Ed.), Volcanism Associated with Extension in Consuming Plate Margins. Geological Society London Special Publication, vol. 81, pp. 115–134.

Van der Laan, S.R., Arculus, R.J., Pearce, J.A., Murton, B.J., 1992. Petrography, mineral chemistry and phase relations of the basement boninite series of Site 786, Izu–Bonin forearc. Proceedings of the Ocean Drilling Program Scientific Results, vol. 125, pp. 171–201.

White, R.V., Tarney, J., Kerr, A.C., Saunders, A.D., Kempton, P.D., Pringle, M.S., Klaver, G.T., 1999. Modification of an oceanic plateau, Aruba, Dutch Caribbean: implications for the generation of continental crust. Lithos 46, 43–68.

Winchester, J.A., Floyd, P.A., 1977. Geochemical discrimination of different magma series and their differentiation products using immobile elements. Chemical Geology 20, 325–343.

Zindler, A., Hart, S., 1986. Chemical geodynamics. Annual Review of Earth and Planetary Sciences 14, 493–571.